AN ABSTRACT OF THE THESIS OF

Donald George Lewis for the degree of DOCTOR OF PHILOSOPHY

in Biochemistry and Biophysics presented on May 27, 1976

Title: CIRCULAR DICHROISM OF AMYLOSE AND GLUCOSE OLIGOSACCHARIDES IN THE VACUUM ULTRAVIOLET

Abstract approved: Redacted for Privacy

W. Curtis Johnson, Jr.

The circular dichroism spectra of amylose, the maltose oligomers, cellobiose, and the cycloamyloses are measured in aqueous solution to 1640 Å. Two bands are found in this region. The long wavelength band is assigned to the ether chromophores; the short wavelength band is assigned to the hydroxyls and further ether transitions. An examination of chromophorically equivalent but conformationally different glucans demonstrates that the circular dichroism of glucans is sensitive to conformation. However, the conformation of the subunits in the maltose oligomer series is independent of chainlength. The conformation of the interior maltosyl groups of this series are all approximately equivalent, and the conformation of the end groups are the same for each oligomer and only one glucosyl subunit in length.

A comparison of the amylose and cycloamylose spectra indicates that amylose is substantially biased in its chirality. Since there is no

chain length dependence, the oligomers must have the same chirality bias.

The data of this study is consistent with conformational calculations on amylose which predict that the maltosyl subunits of amylose are restricted to a small region on its conformational map which includes the V form helix. The butanol complex of amylose, which is believed to have a V form helical conformation, has a circular dichroism similar to free aqueous amylose, indicating that maltosyl subunits of amylose are approximately equivalent for these two species. However, since heated amylose is precluded from having a helical conformation, the temperature insensitivity of the free amylose spectra shows that the maltosyl subunits of amylose are not identically V form. This is consistent with a model for amylose which forms a loose extended helix.

# Circular Dichroism of Amylose and Glucose Oligosaccharides in the Vacuum Ultraviolet

by

Donald George Lewis

A THESIS

submitted to

Oregon State University

in partial fulfillment of
the requirements for the
degree of

Doctor of Philosophy

Completed May 1976

Commencement June 1977

APPROVED:

Redacted for Privacy

Associate Professor of Biochemistry and Biophysics
in charge of major

Redacted for Privacy

Chairman of Department of Biochemistry and Biophysics

Redacted for Privacy

Dean of Graduate School

Date thesis is presented May 27, 1976

Typed by Clover Redfern for Donald George Lewis

TO MY PARENTS,

RALPH AND RITA LEWIS

TABLE OF CONTENTS

## LIST OF FIGURES

# PROLOGUE

The earliest existent example of extended Roman prose is a work by Cato, De Agri Cultura (De Re Rustica) (1). The work was written as a manual for Roman farmers. It has survived because of its utility and simplicity. Section 87 of De Agri Cultura gives a recipe for leaching starch (amylum) from grain. The word amylum comes from the Greek αμυλον (starch) which means "un-milled". Amylum was considered a special form of flour. Amylum contained the whole starch component and possibly some gluten; for it was common to make "pudding cake" from it. Hippocrates recognized therapeutic uses of αμυλον in the treatment of disease. Aristotele recognized the high nutritional energy value of αμυλον.

Starch remains important today because of its many applications and its nutritional value. U.S. patents granted to the food industry and to the materials industry for applications involving amylose are numerous. Such common problems as the staling of bread or the weeping of pudding can result from the retrogradation of amylose. The film or coating properties of starch and its adhesive qualities have found wide application in the materials industries (e.g., paper and textiles), in pharmaceuticals, manufactured food, and industrial processes. The commercial uses and potential applications of starch and amylose are numerous. The total economic impact is substantial.

A field of grain may be thought of as a starch factory. Not fully understood is the starch synthesis mechanisms within the plastid, its transport and deposition upon the starch granule, and its eventual retrieval. Answers to these questions will help the Green Revolution to advance starch husbandry and to develop strains of the highest efficiencies.

Carbohydrate chemistry and the biology of starch are converging to an understanding of the molecular biology of starch. There is a wide variation of starch granule morphology among different plant sources. Also, different granule forms are found within the same plant source (2). In addition, starch granule morphological variation is seen within different strains of the same plant species (3, 4, 5). Morphological schemes for the starch granule or amyloplast usually include a hilum surrounded by birefringent layers or shells of amylopectin-amylose micelles laced together with amylose strands. However, the population, development, composition, size, shape, anatomy, and fate of the starch granule varies. The starch granule is sensitive to alterations of the solvent pH, ionic strength of specific ions, and the hydrogen bond breaking character of the solvent. The introduction of any number of complexing agents can cause conformational and solubility changes in the starch. Recently, an $8_1$ helix complex of amylose was found to form unusual lamallae in solution (6). Steeping in pure water, the granule core swells first as the amylose

core dissolves and retrogrades *in situ*; steeping in hydrogen bond breaking solvents, the amylopectin shells gel first leaving a somewhat stable amylose core (7). A detailed molecular mechanism for these phenomena has not yet been fully elucidated.

Presented in the first part of this paper are the results of the circular dichroism measurements in the vacuum ultraviolet of aqueous solutions of amylose and of various glucose oligosaccharides. This study is novel because the optically active transitions of unsubstituted carbohydrates occur only in the previously inaccessible vacuum ultraviolet region. The study is significant because new conformational information is exhibited in the circular dichroism spectra.

# CIRCULAR DICHROISM OF AMYLOSE AND GLUCOSE OLIGOSACCHARIDES IN THE VACUUM ULTRAVIOLET

## INTRODUCTION

A glucan is any polysaccharide that yields only glucose upon hydrolysis. Amylose and the glucose oligosaccharides are glucans. Amylose is an essentially unbranched α-1-4 glucan polymer found in starch. The shorter linear α-1-4 glucans form the maltose oligomer series (Figure 1). The distinction between the α-1-4 glucan polymer and oligomer is not wholly semantic. Physical properties of the oligomers are functionally more sensitive to chain length than are the amylose polymers (8, 9, 10, 11). The linear α-1-4 glucan oligomers are usually found as a degradation product of the polymer. The cyclic α-1-4 glucans are called Schardinger dextrins. They range in length between six and ten glucosyl units (11). Schardinger dextrins are produced by bacteria. The cyclic α-1-4 glucans are able to complex with a wide variety of compounds. Each of the α-1-4 glucans is isotactic, i.e., neighboring glucosyl subunits are oriented similarly. On the other hand, the β-1-4 glucans are syndiotactic, i.e., neighboring glucosyl subunits are oriented oppositely. Cellobiose is the disaccharide member of this latter class; cellulose is the polymer. Cellulose is a major component of wood.

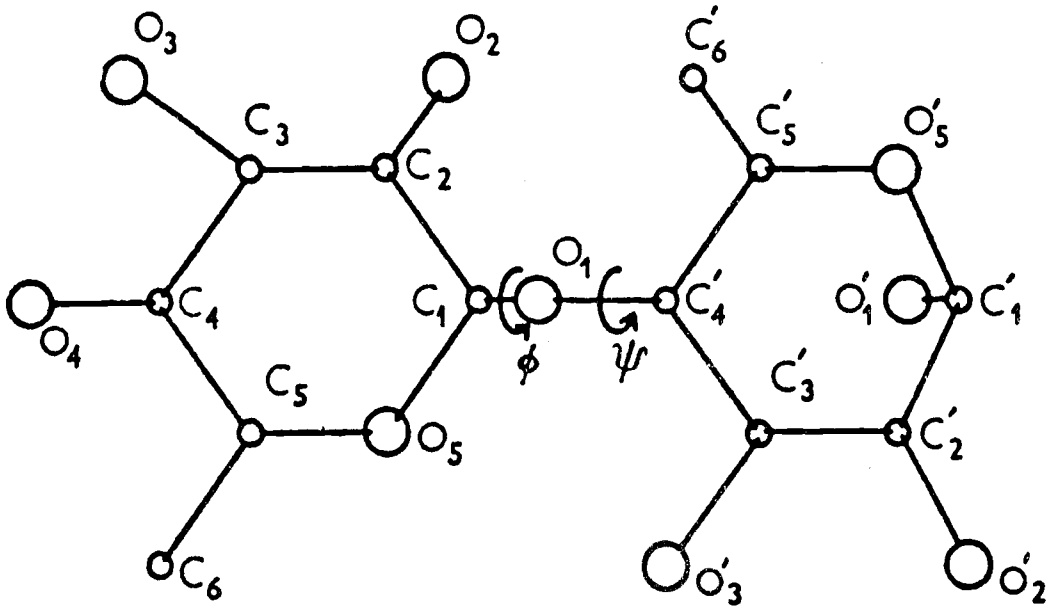


Figure 1. Diagrammatic representation of the maltose residue (with O(6) and O(6') omitted) showing the numbering of the atoms and the angles of rotation $\phi$ and $\psi$ for the two residues. The residues are in the $(\phi, \psi) = (0, 0)$ position (from J. Blackwell, A. Sarko, and R.H. Marchessault [12]).

Solution studies on glucans have been numerous. These studies have utilized spectroscopic and rheological techniques. Several calculations on the solution conformation of glucans have also been published. The history of both the experimental work and the calculations on glucan solutions has been one of increasing sophistication and improvement with each successive investigation.

Both optical rotation and optical rotatory dispersion from the visible to the far ultraviolet have been utilized in previous investigations of the glucans (13, 14, 15, 16, 17). However, circular dichroism bands for the unsubstituted glucans occur only in the previously inaccessible vacuum ultraviolet. The optical rotatory dispersion is observed throughout the ultraviolet and into the visible; the Cotton effects are confined to the vacuum ultraviolet and had not hitherto been observed.

A recent calculation using only optical rotation data at the sodium D-line and crystal structures determined by x-ray diffraction deduced solution conformations for several glucans (18). The results were not entirely consistent. Future efforts along this line can now be improved by eliminating or improving assumptions concerning the bands responsible for the dispersion phenomena. The empirical interpretation of optical rotatory dispersion (ORD) data concerning chain length dependence (13), temperature effects (15, 16) and solvent

perturbations (16, 17) of glucans can be improved in light of the present work.

Induced optical activity and perturbation of electronic transition energies have been utilized to study the complexation of ligands to glucans (9, 10, 19, 20, 21, 22, 23, 24, 25). The induced optical activity or perturbation of the electronic transitions of the complexing agent is thought to be due to the introduction of the complexing agent into either an interior channel of helical amylose or a cavity of the Schardinger dextrins. These assumptions are based upon the solid state location of the ligands. However, the location of the complexing agents in the solid state has some inherent disorder (26).

Induced optical properties are useful in the study of the equilibrium complex and of the complexation process itself. Iodine staining is a useful technique for determining chain length of linear α-1-4 glucans adducts (10, 19, 20, 21, 24). Also, Hamori's spectroscopic studies on the kinetics of iodine binding by amylose have provided insight to the complexation process (22, 23, 25).

Hamori followed the kinetics of the iodine binding by following the time change in perturbation of the electronic transitions of iodine. His findings precluded the earlier random helix model of the conformation of free aqueous amylose. His data indicated that iodine binding was a two step process: 1) nucleation (slow), and 2) propagation (fast). Also it was observed that this same two step binding

occurred even during a second binding episode, i.e., equilibrated regions of bound iodine do not act as nuclei. The fast propagation step could not be reconciled with the earlier random coil model of free aqueous amylose. It was thought that a random coil could not realign itself sufficiently fast to be consistent with the fast propagation rate constant. Also, the inability of equilibrated bound iodine to act as a nucleus during a second binding episode could not be reconciled with the random coil model.

Rheological studies indicate that amylose is a polymorph in solution (e.g., 27, 28, 29, 30). The viscosity of amylose is sensitive to its conformation and this conformation can change with solvent conditions. For instance, amylose becomes more compact upon complexation (23). On the other hand, destruction of the hydrogen bonding potential of the solvent causes the amylose to become more flexible (31).

Hamori's studies (23) on the viscosity of amylose and its iodine complex were very significant for two reasons. His findings cleared up several conflicting reports in the literature. He found that the method of iodine addition was critical to the resultant viscosity. Also his findings that the intrinsic viscosity declines significantly upon complexation precludes the helix or broken helix models of the conformation of free aqueous amylose.

X-ray diffraction studies on amylose and its complexation adducts have shown amylose to be very much a polymorph in the solid state. One x-ray diffraction study investigated 45 different complexation adducts (32). The investigation was not exhaustive (33). Thus far the complexed form has been denoted V form. The V forms have been reported with six, seven, and eight glucosyl units per turn of helix (6, 32). Interconversions among the complexation agents are possible within the solid state (32). Changes in the number of glucosyl units per turn of helix may accompany the interconversion of complexing agent. The V form helices may have either a hydrated or anhydrous form (34, 35). Also possible are interconversions in the solid state between the V forms and B forms (36). B form amylose is not complexed; but it is greatly hydrated and extended (12). The B form may vary between four and six glucosyl units per turn (37). The retrogradation product of amylose standing in aqueous solution is a B form helix. There is speculation that interconversion is possible in the solid state into any V or B form unless the interconversion requires a change in chirality (38). There is evidence that some helical forms are unstable with time and require annealing (39). Butanol precipitated amylose was one of the first biological macromolecules to be investigated by x-ray diffraction (40). Progress in the elucidation of its structural geometry has been slow (35). The potential for x-ray diffraction studies on further forms of the amylose

polymorph is substantial and promising.

X-ray diffraction studies on oligomeric glucans have been more definitive (24, 41, 42, 43, 44, reviewed 45). The solid state structure of the glucans has been clearly elucidated. The dimensions and angles of the glucosyl subunits as given by the x-ray studies have been utilized in most theoretical studies on the solution conformation. Unfortunately, the critical glucosidic linkage angle and rotational angles can not be taken from the x-ray work. They will require further evidence from solution studies to be determined (18).

Several workers have made energy calculations on the conformational space of various glucans resulting in Ramachandran type maps in $\phi$ and $\psi$ (36, 44, 46, 47, 48, 49, 50). The maps from the various calculations differ in the details of the lowest energy regions but agree in gross characteristics. The results from one early maltose calculation by Marchessault is reproduced in Figure 2 (44). The dotted line on Figure 2 represents the outer limit for the low energy conformational space for maltose. This map is largely in agreement with later calculations for maltose.

The conformational maps of glucans are divided into the two chiralities at the $h = 0$ line. The area below the $h = 0$ line in Figure 2 yields a left handed helix and the area above the $h = 0$ line yields a right handed helix. Figure 2 shows that the $h = 0$ line bisects the occupied conformational space of maltose. A later

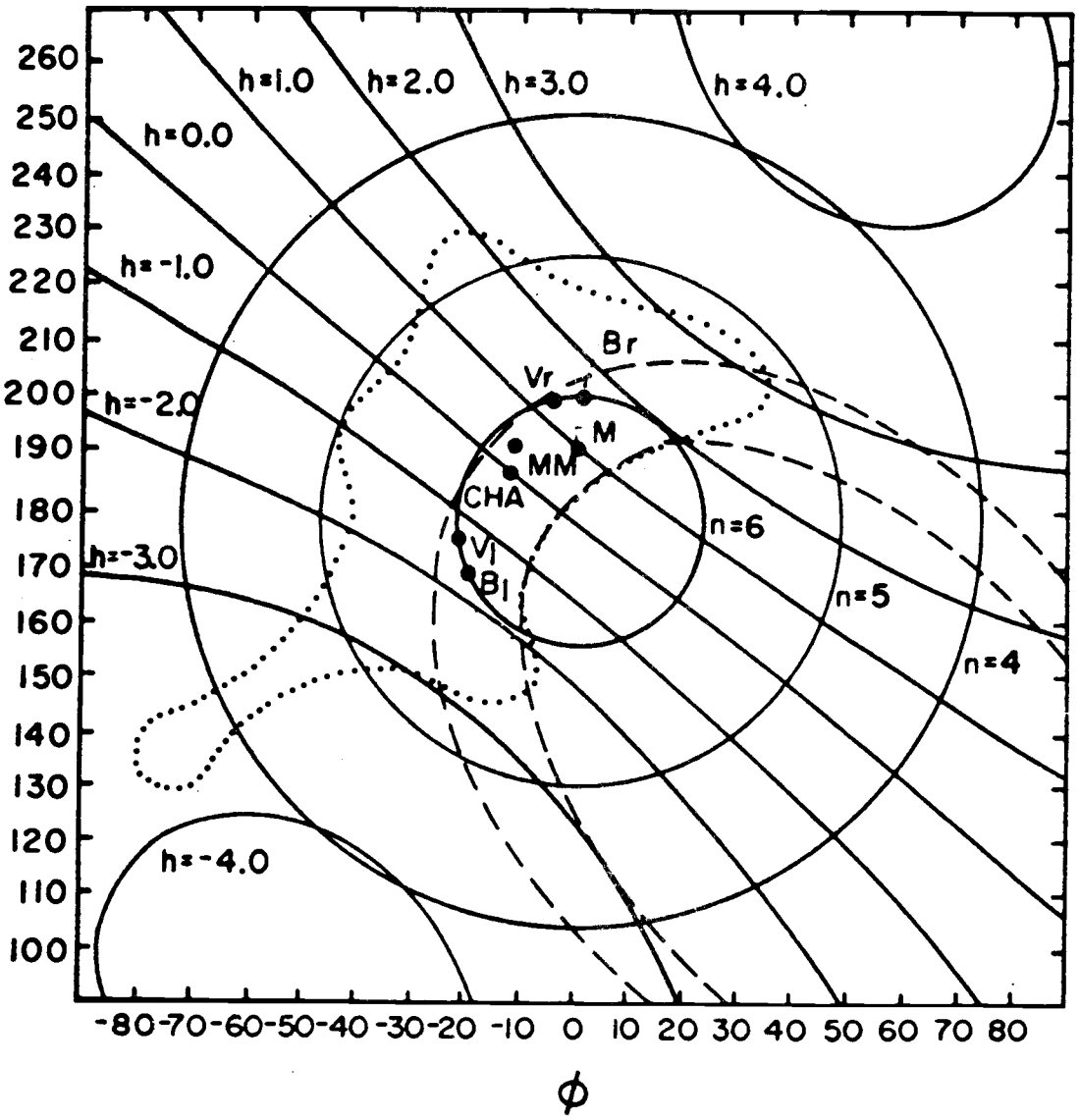


Figure 2. Allowed conformational region (dotted line) for maltose with a bridge angle of 117°. Dashed lines bound the area of acceptable O(2) → O(3') hydrogen bond lengths (2.6-3.0 Å). The n and h contours are, respectively, the number of residues per turn of helix and the axial per rise per residue in angstrom units (positive h indicates a right handed helix): M, β-maltose; MM, β-methyl-maltose; CHA, cyclohexylamylose; $V_L$ and $V_R$ left- and right-handed V-amylose; $B_L$ and $B_R$, left- and right-handed sixfold B-amylose (from G. J. Quigley, A. Sarko, and R. H. Marchessault [44]).

calculation by Brant, claiming greater resolution, assigns 77% of the partition function of maltose to the left handed chirality and 23% to the right handed chirality (50). The calculation of the chirality bias in maltose is critically dependent on the chosen value of the glycosidic angle (50). Increased temperature will tend to broaden the distribution of the glycosidic angle. This has the effect of destroying the chirality bias. Thus, increased temperature is expected to destroy the chirality bias of maltose (50).

The Ramachandran map of maltose is unusual. Maltose has only one occupied energy minimum, comparatively broad. Ramachandran maps of the dimeric member of other classes of polymers usually contain multiple low energy regions. Also it is unusual that the occupied conformational space of the maltose dimer straddles the $h = 0$ line. The energy difference between the two chiralities of maltose is small and a transition from one chirality to the other is unhindered.

A singular feature dominates the transformation on the Ramachandran maps on going from the maltose dimer to the amylose polymer. A potential barrier arises along the $h = 0$ line. This potential barrier increases with oligomeric chain length until penetration of the barrier becomes an impossible mechanism for the transition of chirality of the amylose polymer. The $h = 0$ line represents the degenerate helix form as in the cycloamyloses. Brant has

proposed a mechanism for a chirality transition in amylose which avoids the $h = 0$ line (49). It is proposed that the energetically most favorable route for the chirality transition is through the extended helix form.

While the potential barrier separating the two chiralities of amylose is very large, the energy difference between the minima of either chirality is small. Brant's calculation puts this energy difference at 2.6 kcal/mole, near the limit of its uncertainty (49). This calculation favors the left handed chirality as the low energy form. However, this is near the present limit of resolution for such calculations.

All of the various Ramachandran type calculations for the α-1-4 glucans entail approximations of some degree. None of the calculations consider the contributions of water structure about the glucan. The direction or existence of a chirality bias in amylose or its oligomers has not been unequivocally established by any of the various energy calculations.

One notable result of all the energy calculations on the glucan conformational map is that the low energy space of the polymer is always much more narrow and deep than that of maltose. These calculations all prodict that the conformational freedom of the polymer is more restricted than that of maltose.

For many classes of polymers in solution, the ordering of a helical state effects substantial lowering of energy at that singular point on its conformational map. Although the conformational maps of amylose are highly restricted in the low energy region, singularities are missing. Calculations on the conformational map of amylose do not point to a singular helical form as the dominant form (see Brant, 50). By this model, the conformation of amylose in aqueous solution is greately restricted on a local level but is not helical. The restricted low energy regions of amylose do include some helical points. It is thought by Hamori (22, 25) that upon complexation, the conformational map of amylose narrows to one such singularity, i.e., the amylose becomes helical. Thus a gross conformational change upon amylose complexation is accompanied by a small change in the conformational map. The narrow restricted occupied region of amylose shrinks to a singularity within the region upon complexation.

# EXPERIMENTAL

## Materials

Circular dichroism measurements were made on amylose; four linear α-1-4-glucosyl oligosaccharides: maltose, maltotriose, maltotetraose, and maltopentaose; two cyclic glucosyl oligosaccharides: cyclohexylamylose (Schardinger's α-dextrin) and cycloheptylamylose (Schardinger's β-dextrin); and the β-1-4-glucosyl disaccharide, cellobiose. All materials were purchased from commercial sources.

Circular dichroism measurements were made on both Type I and Type III potato amylose purchased from Sigma Biochemical Co. Type III amylose is prepared by thymol precipitation and is amylopectin free. This amylose requires the solubilization procedure of Hamori (30) which consists of an initial wetting of the amylose with ethanol, adding boiling water, refluxing for an hour under an inert atmosphere, and then centrifuging down the undissolved particles. Unfortunately, the 1 percent ethanol of the final solution prevented measurements below 1840 Å. To extend the spectrum further, Type I amylose was used. It could be readily solubilized without the ethanol wetting step so that the spectrum could be measured to 1650 Å. Although Type I amylose (purified by a single butanol precipitation) contains 5 percent amylopectin, its spectrum is

superimposable with Type III.

The molecular weight distribution of potato amylose is broad (51). Fortunately, spectroscopic studies are not affected by the use of heterogeneous amylose solutions. Since end effects can be neglected, this heterogeneity has no immediate spectral effect for the long chain amylose (10). This is a decided advantage over viscosity studies which require homogeneous amylose in order to facilitate interpretation. Also, homogeneity has the effect of accelerating the retrogradation process in amylose (8). Thus, spectroscopic studies on amylose are not as troubled by instability as are viscosity studies. Because heterogeneity is characteristic of the native state of amylose, the heterogeneous mixture is the more biologically interesting system to study.

All aqueous solutions of amylose retrograde at some rate. The Sigma Type III amylose, first solubilized with ethanol and then complexed with butanol, was only stable enough to allow one measurement for each preparation. However, all other solutions were more than sufficiently stable over the times of the measurements. Stability against retrogradation was indicated by the consistency of the spectra with successive rescanning and of the viscometric measurements described infra. Retrograded solutions were opalescent and their transmission spectra changed with time.

The Sigma Type I amylose solutions had concentrations varying between 0.1 and 1 percent. Because of limitations within the solubilization procedure, the Sigma Type III amylose solution was made to only 0.3 percent.

Solvents for the amylose include both $D_2O$ and $D_2O$-n-butanol mixture. $D_2O$ is preferred over $H_2O$ because of its greater transparency into the vacuum ultraviolet. N-butanol is known to form a complex with amylose (22, 30, 52). The complex is thought to organize the normal amorphous amylose solute into a helical form. In any event, viscometric studies show that the reduced viscosity is decreased upon complexation such as to indicate a contraction of the amylose. The n-butanol was Matheson, Coleman and Bell spectroquality. The amylose-butanol solutions were made five percent butanol of the final solution volume. At about eight percent by volume butanol, the two solvents separated into different phases and also at about this mixture the amylose quickly precipitated. Butanol fractionation is of course the classic way of isolating amylose from the whole starch. At five percent butanol, the viscosity number has suffered approximately half of its diminution on going from aqueous to the butanol precipitate. If one extrapolates from a kinetic study on a complexing agent yielding a helical form identical to the butanol precipitate, viz, iodine (22), the the diminution of the viscosity number indicates that the fraction of amylose in the complexed form is

substantial--approximately half. Viscometric measurements were made to verify the reduction of viscosity number upon butanol complexation as reported in the literature (52).

The maltose and cellobiose were purchased from both Pfanstiehl Laboratories, Incorporated and Pierce Chemical Company. The maltotriose was purchased from both Kock-Light Laboratories Ltd. and Pfaltz and Bauer. The maltotetraose was purchased from both Kock-Light Laboratories Ltd. and Pierce Chemical Company. The maltopentaose was commercially available from Pierce only. Spectral measurements were found to be consistent for the different sources of each of the linear glucans.

Cyclohexylamylose (Schardinger's α-dextrin), cyclohexylamylose-cyclohexane complex, and cycloheptylamylose-cyclohexane complex were each purchased from Sigma Chemicals. The low solubility and heat lability precluded a study of the cyclohexane comlexes. The spectra obtained from both cyclohexylamylose samples (the uncomplexed cyclohexylamylose and the cyclohexylamylose prepared by driving off the complexing cyclohexane by briefly heating to boiling under a flushing helium atmosphere) were identical. The cycloheptylamylose was similarly prepared. The cycloheptylamylose-cyclohexane complex is more heat labile than the cyclohexylamylose-cyclohexane complex. Except for the cyclohexane complex factor, the Schardinger dextrins were treated indentically

to the linear glucans.

All carbohydrates investigated were first dried to constant weight under vacuum with phosphorus pentoxide. Typically this required three days. The samples were weighed and dissolved in $D_2O$ to a known volume. Final concentrations varied between 0.1 and 1.0 percent for all of the glucans. Beer's law was verified to be obeyed in each case.

Method

The spectral measurements were made on a vacuum ultraviolet circular dichroism spectrophotometer described elsewhere (53). Temperature variable cells were fabricated and adapted to the apparatus. The temperature dependence of the spectra were measured at 10°C intervals between 10°C and 50°C. The temperatures were measured by means of a thermistor. The thermistor was calibrated under experimental conditions by viewing the freezing of a water filled cell at 0°C. For quantitative work, there were three cells of known light path lengths: 500 μ, 100 μ, and 50 μ nominal. For the cells of the shortest known path lengths, the precise length was determined interferometrically. The cutoff point for the quantitative measurements was approximately 1730 Å. The precise cutoff values depended on the concentration of the solute.

To extend the spectra beyond the cutoff of the quantitative work, a variable path length cell was fabricated. The shortest path lengths were achieved by interposing the solution between two Supersil quartz disc windows pressed together without a spacer. The path length approached 4 μ in length. The cutoff point (where total OD $\leq$ 1) for the shortest path length technique sometimes reached 1630 Å. The $D_2O$-n-butanol mixtures cutoff at approximately 1730 Å, due to the butanol absorption. The cutoff point was determined for all measurements. Spectra obtained by the variable cell technique were matched with their overlap of spectra in the quantitative region.

At the commencement and conclusion of each day's spectrometric work, the vacuum ultraviolet circular dichroism spectrophotometer was calibrated using d-10-camphorsulfonic acid assuming a $\Delta\epsilon$ (2905 Å) value of 2.20. Although there was occasional long term drift in the calibration, it rarely varied by more than one percent or two percent over a day's period. The maintenance of the instrument's sensitivity was an endless exercise. Its chronical would be a compendium for the practicing spectroscopist.

Spectral measurements for amylose, maltose, cellobiose, and the Schardinger dextrins were repeated several times. However, for the higher linear α-1-4 glucose oligomers, a set of measurement were made only once for each commercial source because of their high

cost. The spectral measurements were reproducible to about 10 percent.

For the butanol complexed amylose spectra, viscosity measurements were made to verify the complexation. The method of Banks and Greenwood was used (52). An Ubbelohde dilution type capillary viscometer was used. It was placed in a constant temperature 25°C water filled tank and aligned vertically. Efflux time was 1069 seconds for the amylose solution. Reproducibility was ± 0.2 seconds for amylose and ± 0.6 seconds for the complex. The change of the viscosity number upon complexation was consistent with the observations of Banks and Greenwood indicating that complexation had indeed occurred.

# RESULTS

The circular dichroism of amylose and its oligomers is shown in Figure 3 through 8. In each case, the circular dichroism scale is given as $\Delta\epsilon$/glucosyl unit, i.e., the molecular $\Delta\epsilon$ is divided by the number of glucosyl units in the chain. This facilitates a comparison among amylose and the maltose oligomers. The unique chromophoric contributions attributable to the reducing and nonreducing ends of amylose are vanishingly small and can be neglected. However, the maltose oligomers of differing lengths are anticipated to differ in their circular dichroism spectra because of the varying contributions of end group and interior glucosyls with chain length.

The circular dichroism spectra for amylose in aqueous solution is given in Figure 3. There are two prominent bands: a long wavelength negative band at about 1820 Å and a short wavelength positive band with a maximum to the blue of the spectral cutoff at 1640 Å. The low energy band shifts to the red about 20 Å as the solution temperature is raised from 10°C to 50°C. The magnitude of the band decreases by about 10 percent over the same temperature range. At about 1840 Å, there is an isosbestic point. As the amylose solution is heated, the high energy band also shifts to the red or broadens and declines in magnitude. On the long wavelength side of the 1640 Å band, there is another isosbestic point at about 1710 Å. The 1640 Å

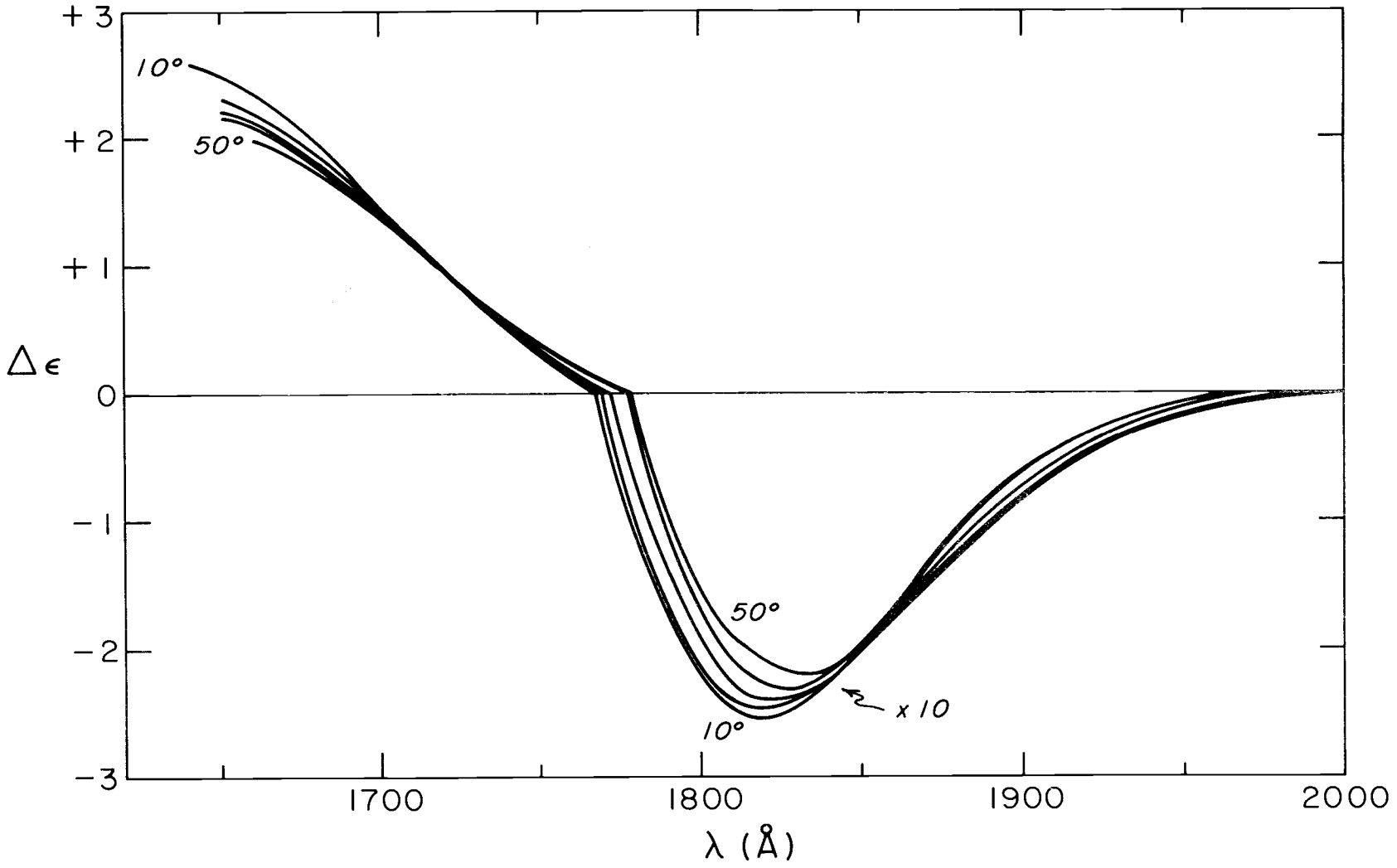


Figure 3. Circular dichroism spectra of amylose at 10°, 20°, 30°, 40° and 50°C.

band is about ten times the magnitude of the 1820 Å band and partially overlaps the 1820 Å band. Its shifting with temperature substantially alters the behavior of the 1820 Å band.

The circular dichroism spectra for a five percent n-butanol-aqueous solution of amylose is given in Figure 4. At a concentration of greater than seven percent n-butanol, the amylose readily precipitates out as bundles of V form butanol-amylose helical complex. In the five percent n-butanol solution, about 50% of the amylose is complexed to butanol (24, 30, 52). The cutoff point was at about 1770 Å due to absorption by the butanol.

A comparison of the aqueous and aqueous-butanol solution spectra of amylose reveals that their behavior and description are very similar. The 1640 Å band shifts to the red or broadens upon heating. The 1820 Å band also shifts to the red and decreases in magnitude upon heating. However, the magnitude of the 1820 Å band for the butanol complex is approximately twice as sensitive to changes in temperature for the aqueous butanol solution.

The circular dichroism spectra of maltopentaose, maltotetraose, maltotriose, and maltose are given in Figures 5, 6, 7, and 8 respectively. Each of these spectra share some common features with the amylose spectra but also exhibit chain length dependent effects. Like amylose, the oligomeric spectra each have a positive short wavelength band at about 1650 Å and a negative long wavelength band at about

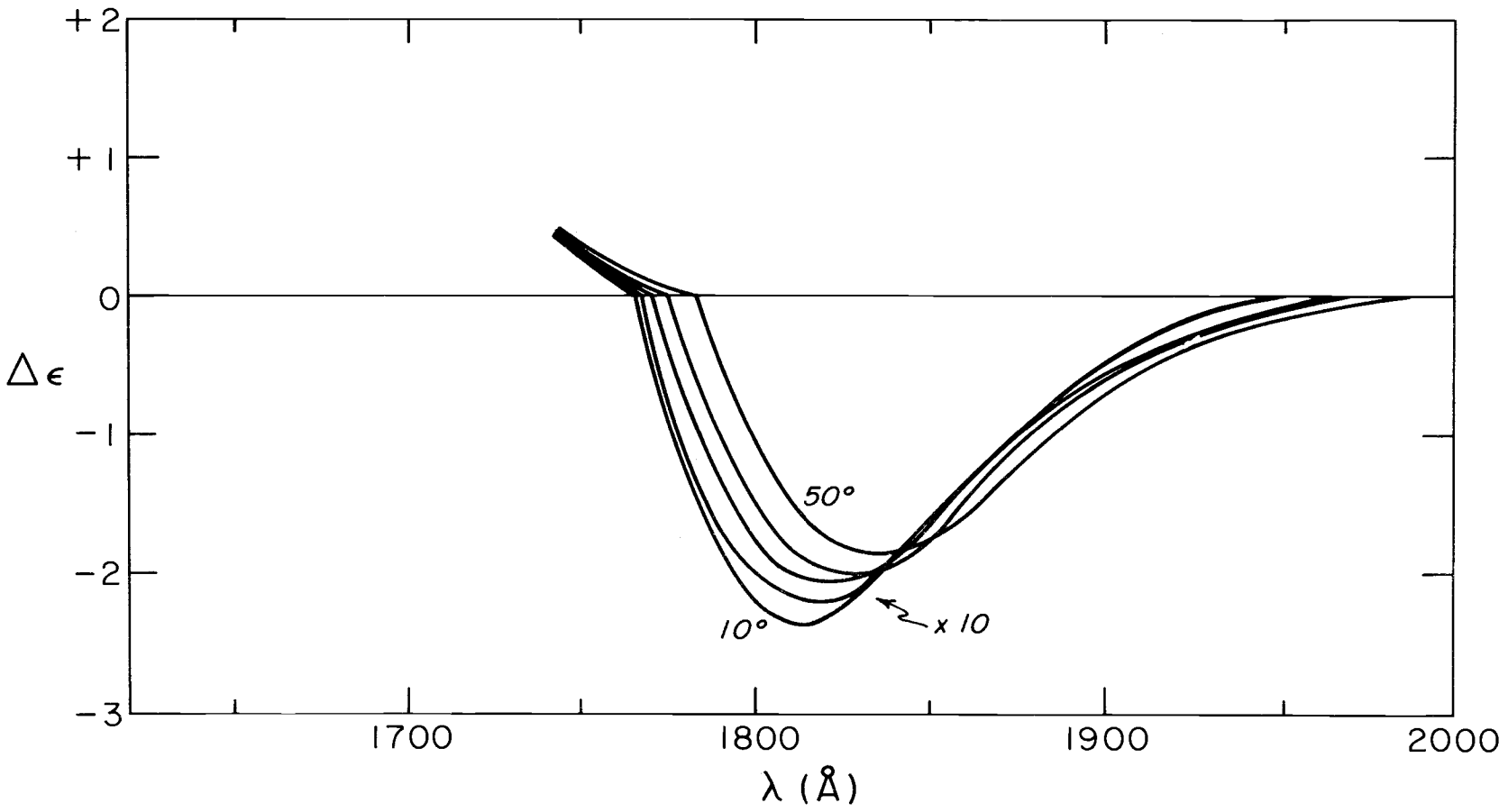


Figure 4. Circular dichroism spectra of amylose in a five percent n-butanol-$D_2O$ solvent at 10°, 20°, 30°, 40°, and 50°C.

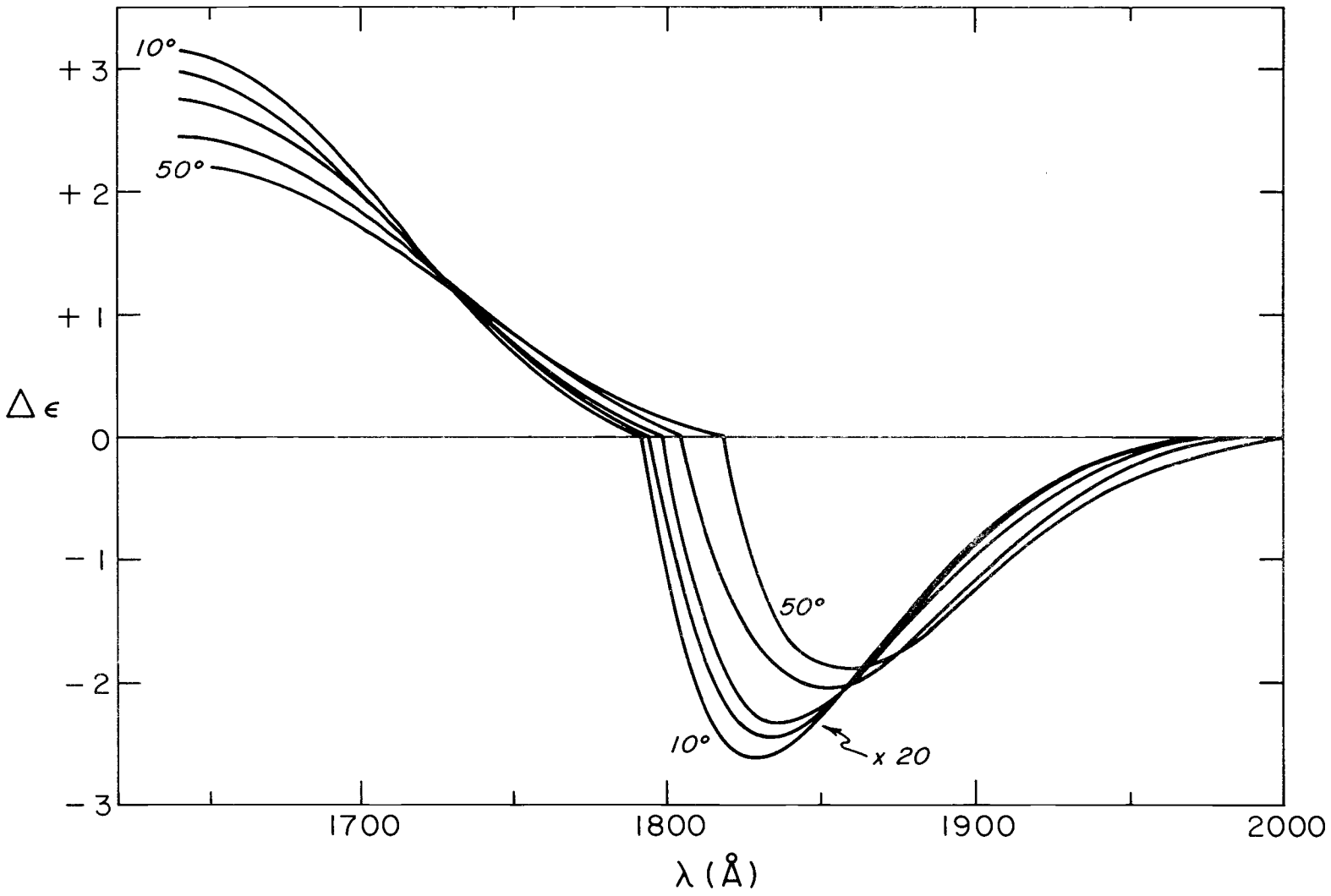


Figure 5. Circular dichroism spectra of maltopentaose at 10°, 20°, 30°, 40°, and 50°C.

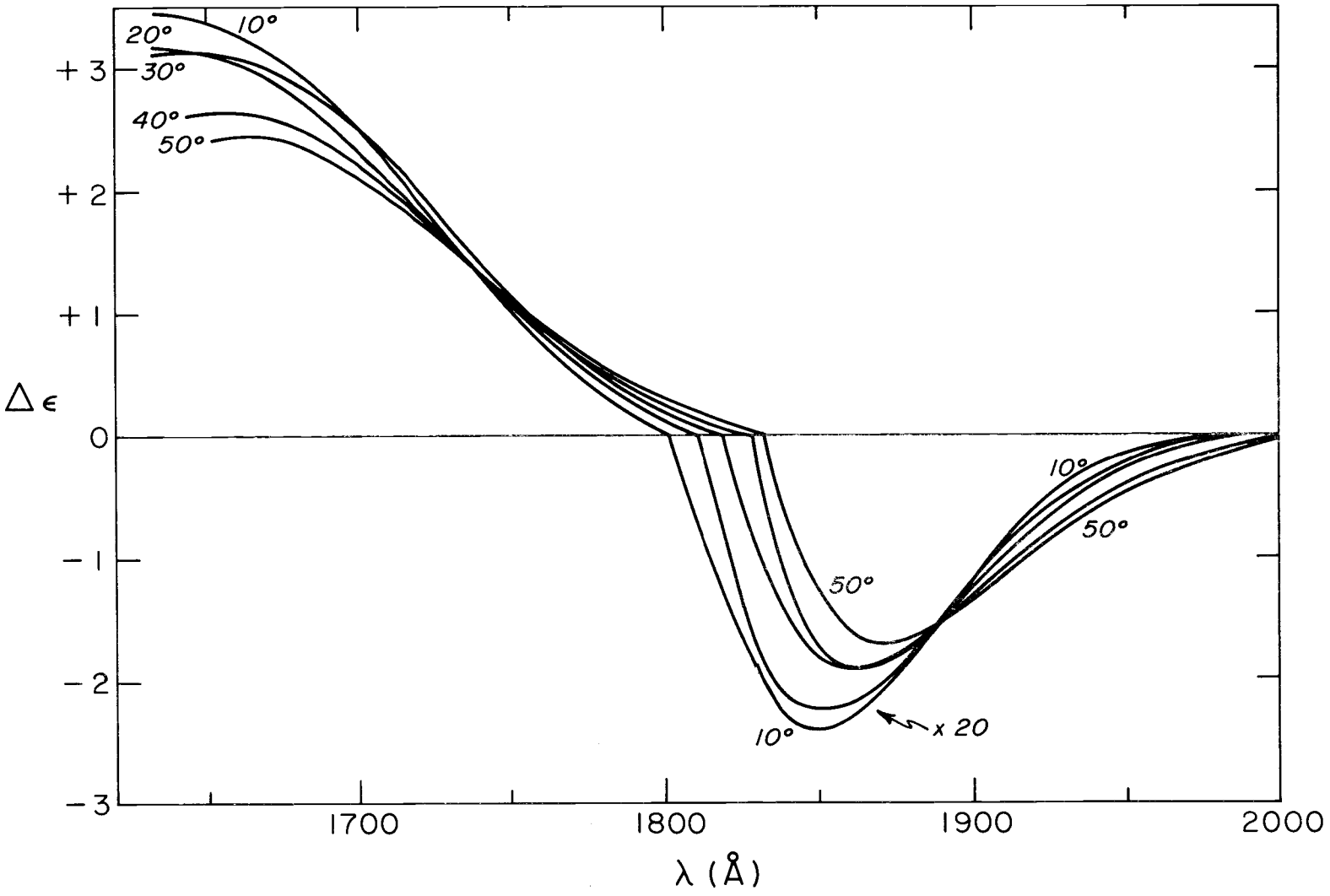


Figure 6. Circular dichroism spectra of maltotetraose at 10°, 20°, 30°, 40°, and 50°C.

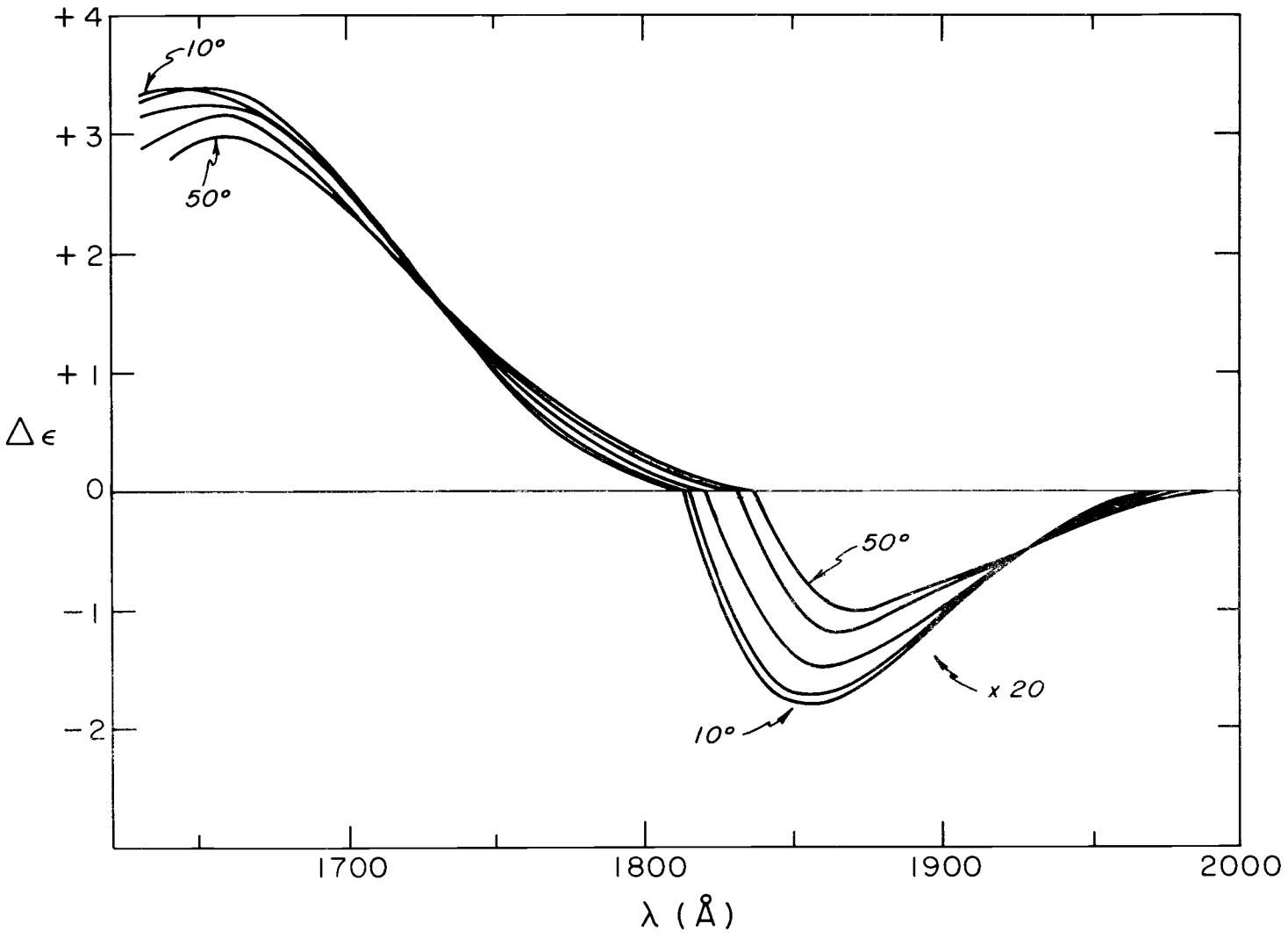


Figure 7. Circular dichroism spectra of maltotriose at 10°, 20°, 30°, 40°, and 50°C.

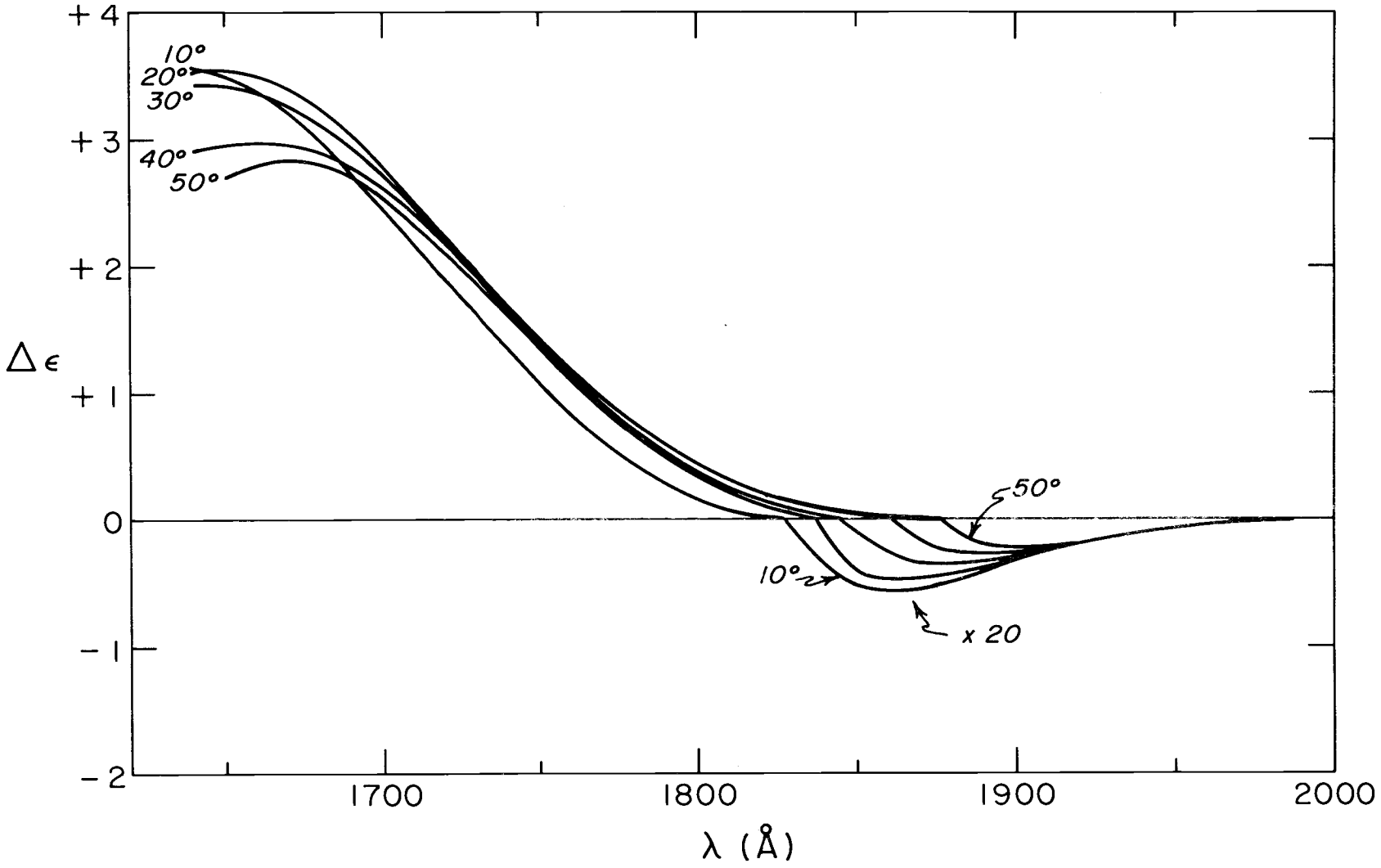


Figure 8. Circular dichroism spectra of maltose at 10°, 20°, 30°, 40°, and 50°C.

1850 Å. The 1650 Å band is always the greater in magnitude. Also, like amylose, all bands shift to longer wavelengths upon heating. When the 1650 Å band of the oligomers shifts to longer wavelengths upon heating it progressively increases its overlap of the 1850 Å band. The short wavelength band maximum is measurable for several oligomers. The band shape of the 1650 Å band of maltopentaose indicates that its maximum is to the red of the comparable band in amylose. The 1650 Å band of maltotetraose, maltotriose and maltose are observed and in each case is to the red of both amylose and maltopentaose. The magnitude of the 1650 Å band is greater for the oligomers than for amylose. The sensitivity to temperature of both bands is greater for the oligomers than for amylose. The magnitude of the 1850 Å band becomes progressively smaller as a function of decreasing chain length. The position of the isosbestic points of the 1850 Å bands progressively shifts to longer wavelengths as a function of decreasing chain length. In maltose the isosbestic point is poorly resolved.

It should be noted that the 10°C spectra for maltose and, to a lesser degree, for maltotriose behave anomalously. The 1650 Å band shifts discontinuously to the blue on going from 20° to 10°C. The 1650 Å band for maltose markedly shifts from the isosbestic point at 10°C.

The circular dichroism spectra of cellobiose is given in Figure 9. Unlike the α linked oligosaccharides, cellobiose has only one band.

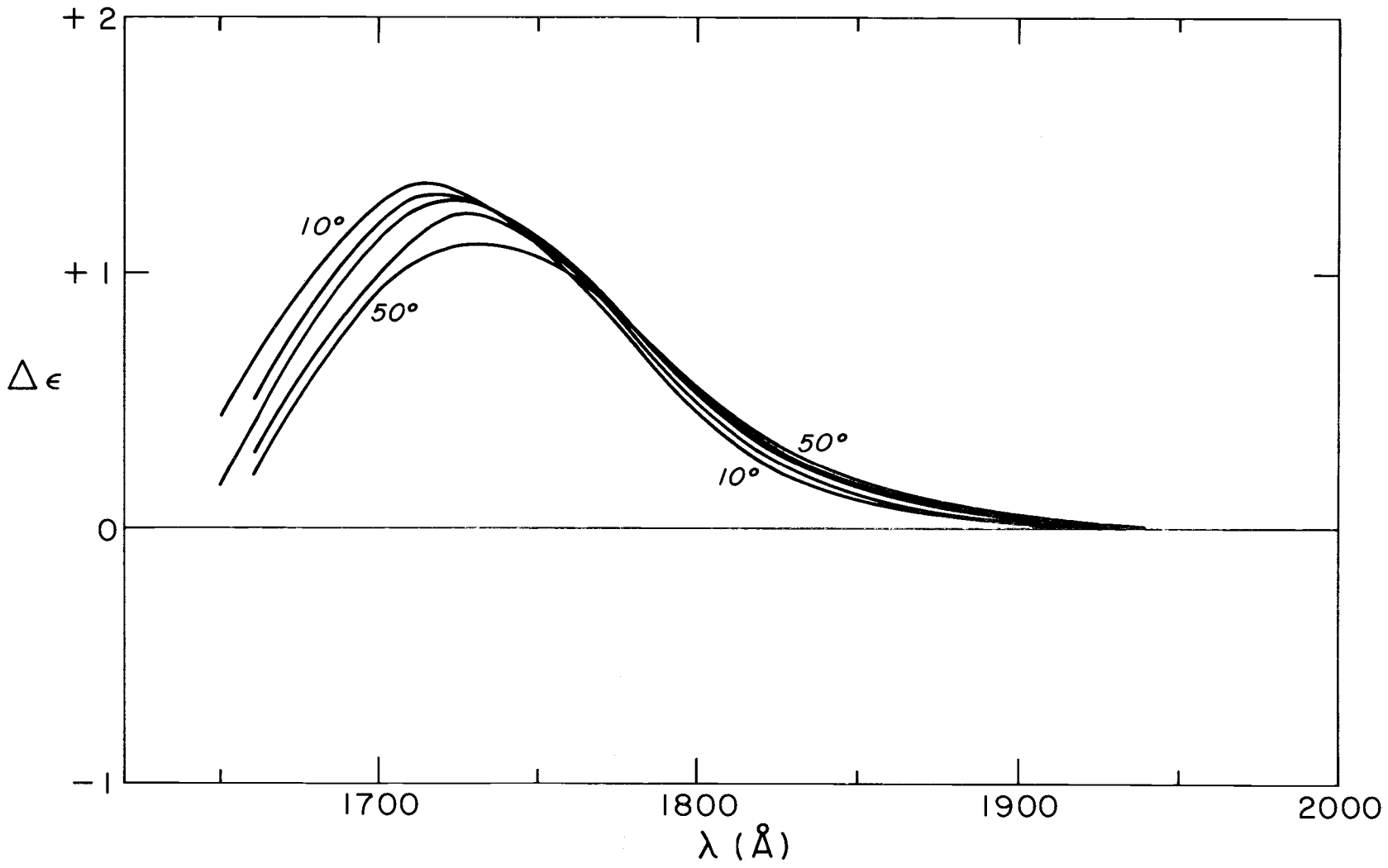


Figure 9. Circular dichroism spectra of cellobiose at 10°, 20°, 30°, 40°, and 50°C.

The band is positive and peaks at about 1720 Å. The band shifts to the red and diminishes in intensity as the temperature increases. The 1720 Å band of cellobiose is comparatively less intense than the α linked oligomers. The 1850 Å band present in the α linked oligomers is missing. It has either changed sign and remained very small or it has shifted to the blue.

The circular dichroism spectra of cyclohexylamylose and of cycloheptylamylose are given in Figures 10 and 11. Like cellobiose they have only one band. The maximum of the band lies to the blue of the 1640 Å cutoff. The intensity of the band is considerably greater than the other short wavelength bands here studied. The intensity of the cycloheptylamylose band decrease monotonically as the temperature increases. However, the intensity of the cyclohexylamylose band increases between 20°C and 30°C but otherwise decreases monotonically with increasing temperature.

The circular dichroism spectra of both anomers of glucose and of an equilibrium mixture of glucose as measured by Richard Nelson is given in Figure 12 (54). Also as measured by Richard Nelson are the circular dichroism spectra of both anomers of the methyl-glucosides in Figure 13 (55). Both anomers of glucose have an intensive positive band below 1700 Å wavelength and both are thought to have a low intensity band at the long wavelength end. The α-glucoside spectrum has three bands. The first band is positive and appears as

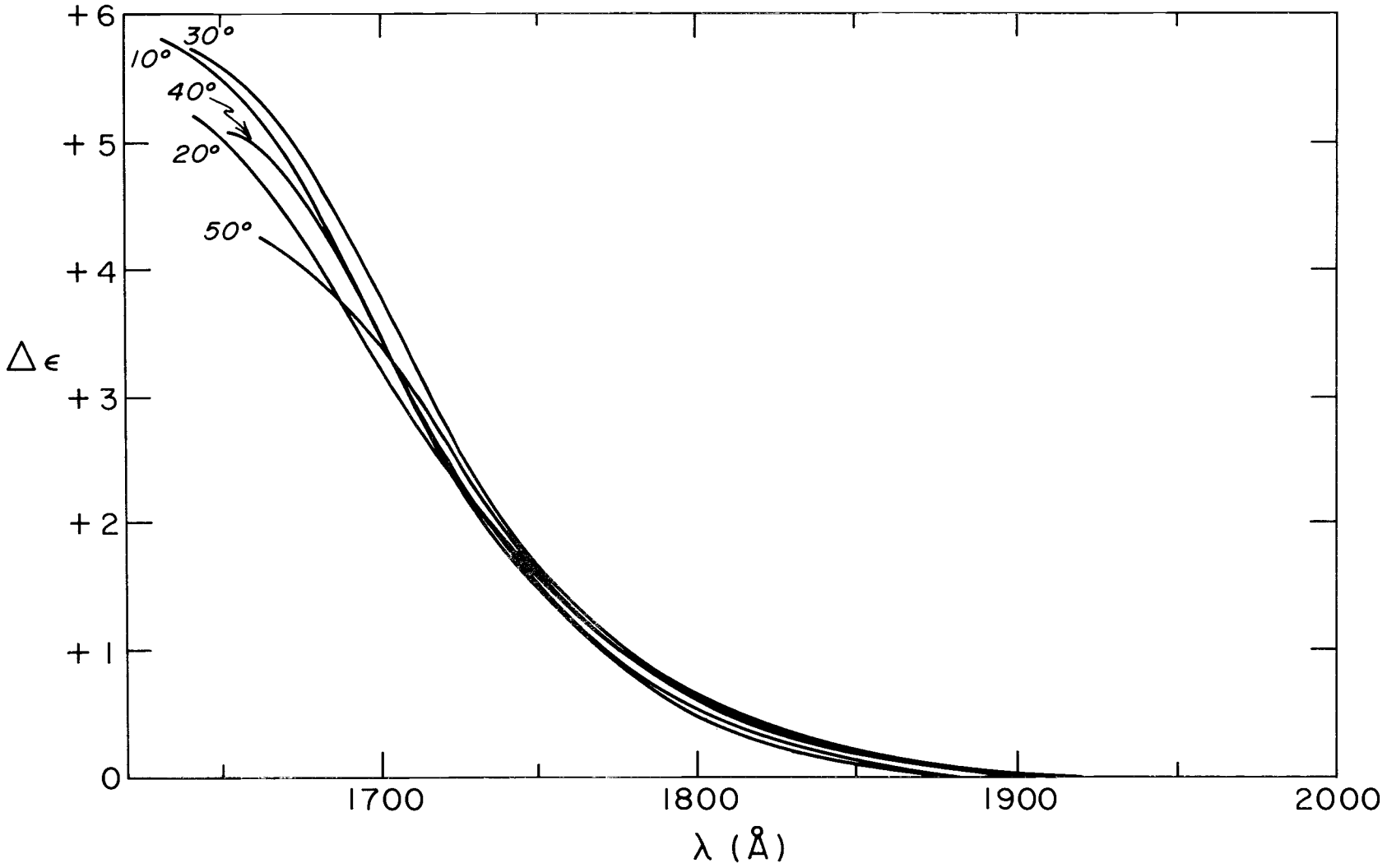


Figure 10. Circular dichroism spectra of cyclohexylamylose (Schardinger's α-dextrin) at 10°, 20°, 30°, 40°, and 50°C.

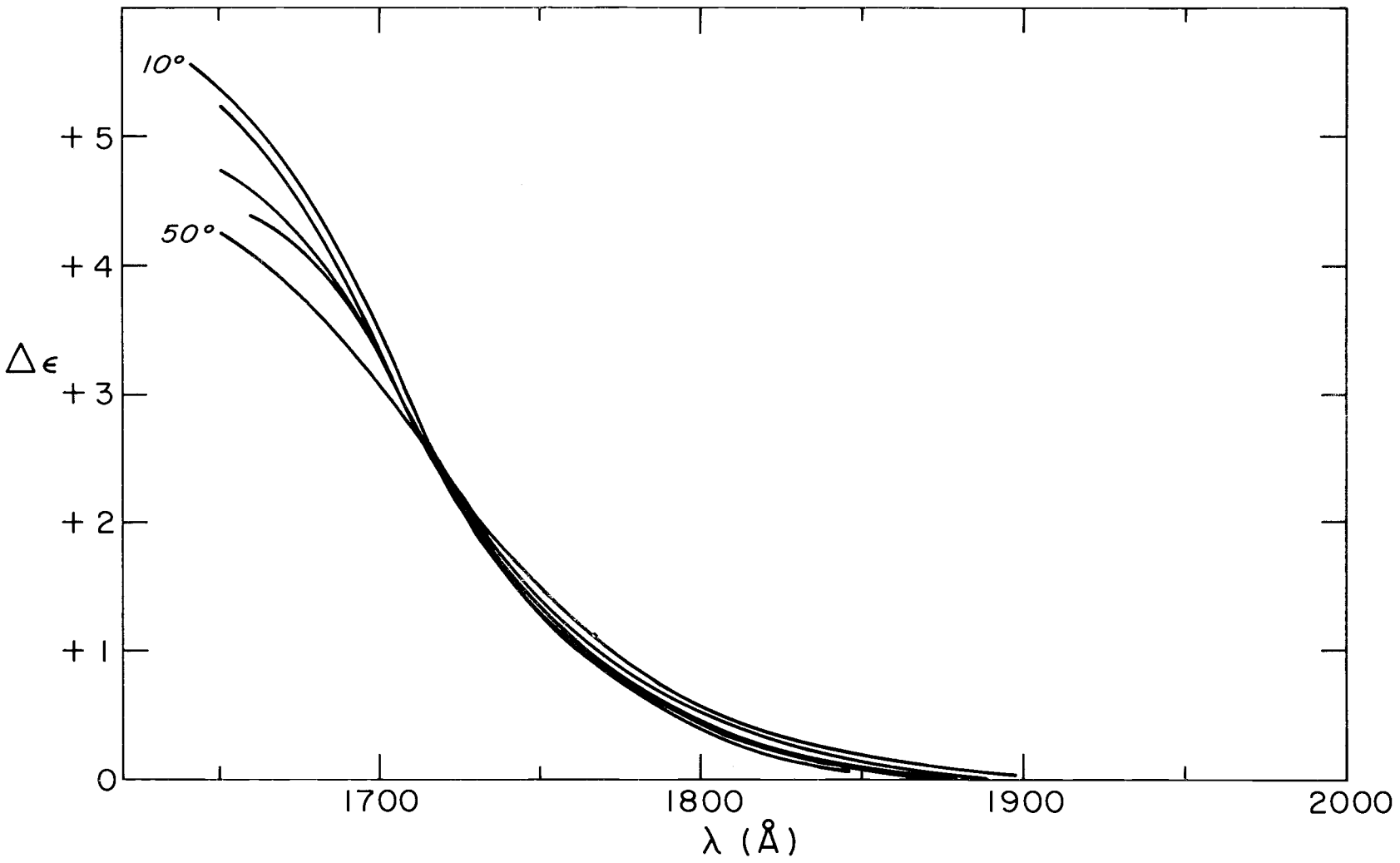


Figure 11. Circular dichroism spectra of cycloheptylamylose (Schardinger's β-dextrin) at 10°, 20°, 30°, 40°, and 50°C.

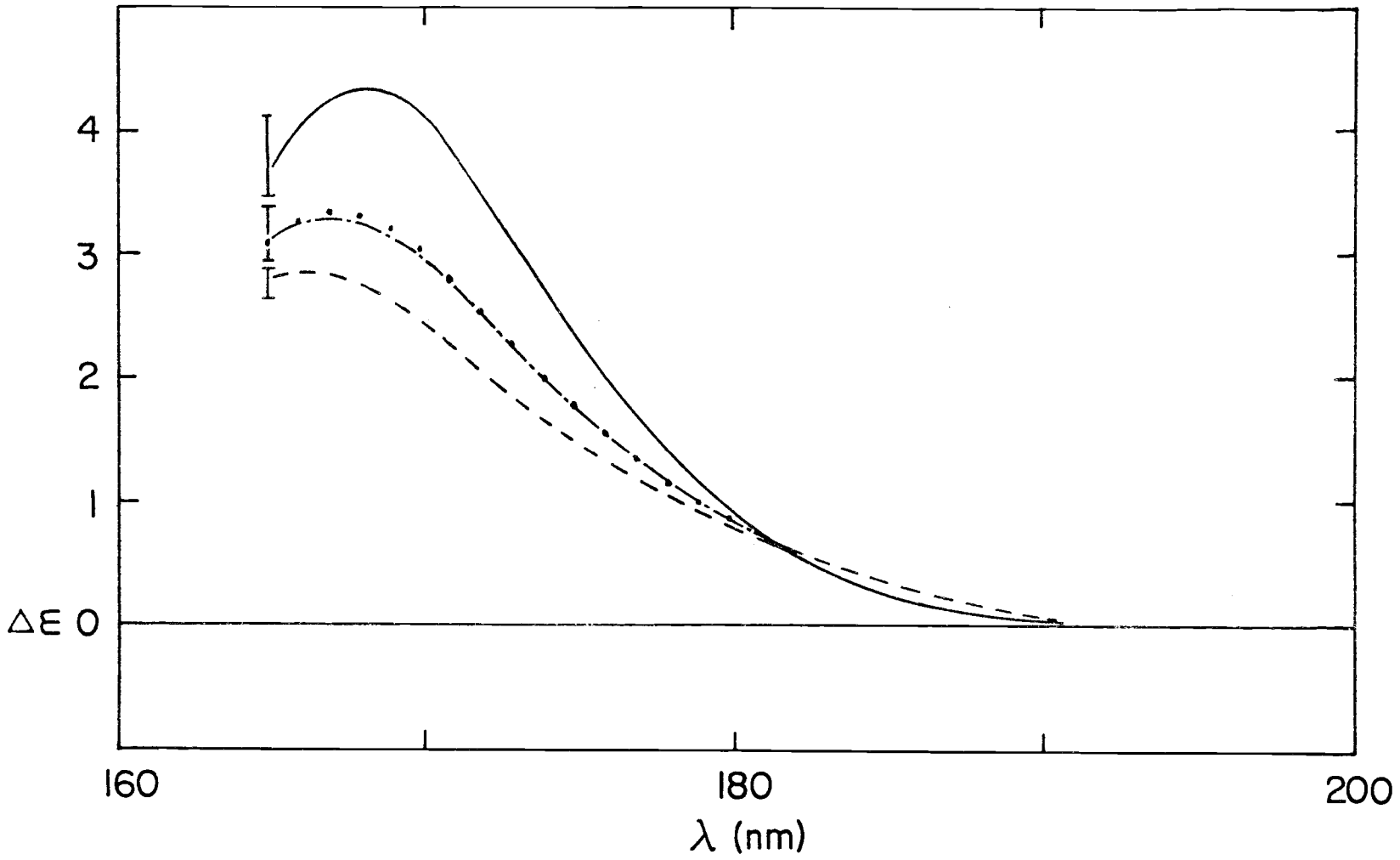


Figure 12. CD spectra of α-D-glucopyranose (——), β-D-glucopyranose (---), equilibrium D-glucopyranose (-·-·-) and calculated equilibrium D-glucopyranose (ooo).

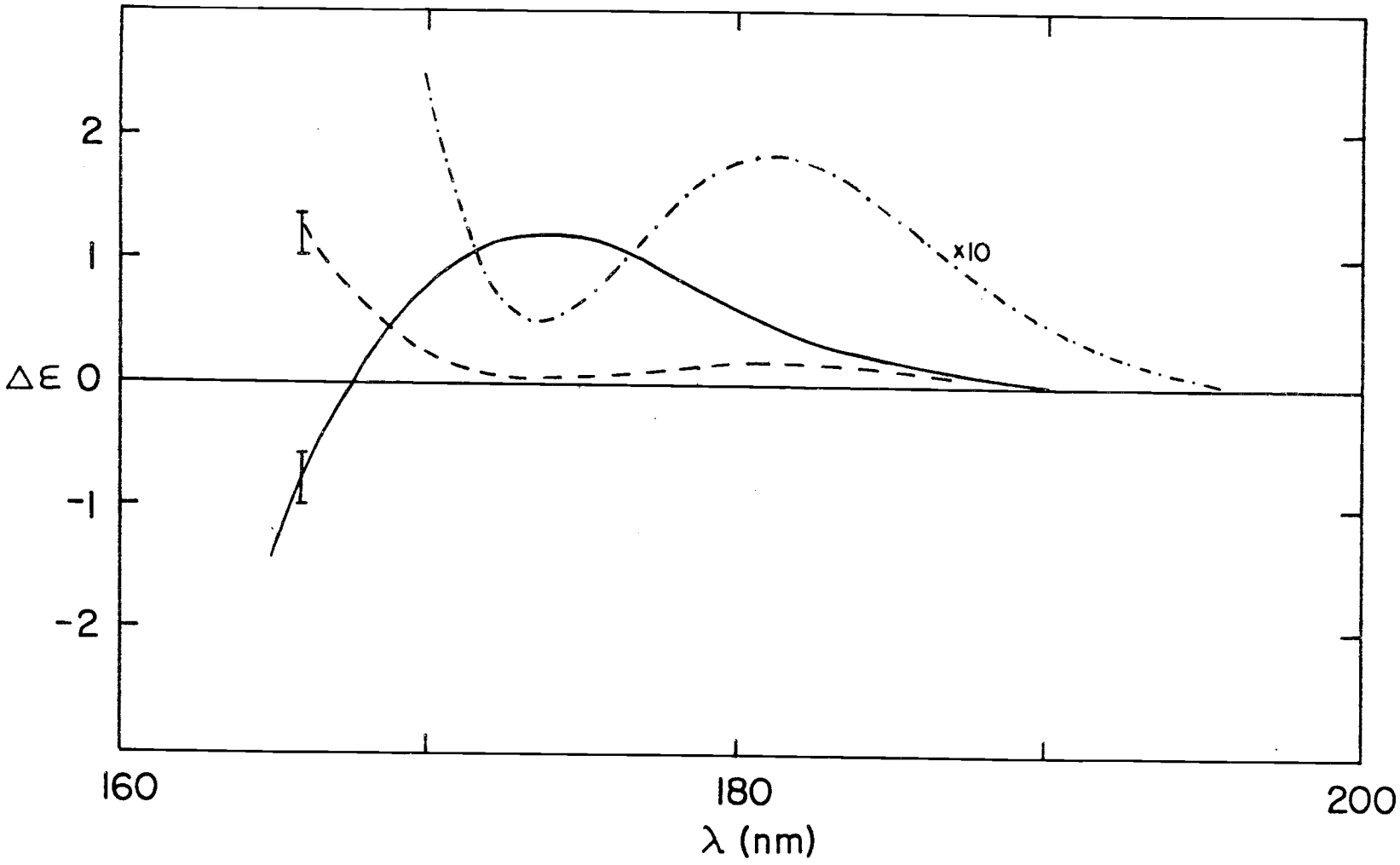


Figure 13. CD spectra of methyl α- (——) and β- (---) D-glucopyranoside.

a low intensity tail at the long wavelength end of the spectrum. The second band is also positive, of intermediate intensity and lies at about 1740 Å. The third band is negative, rather intense and lies below the cutoff of 1640 Å. The β-glucoside has a positive low intensity band at 1820 Å and a more intense positive band lying below the 1650 Å cutoff.

# DISCUSSION

## Assignment of Transitions

Earlier work on monosaccharides, glycosides, and model sugar compounds showed that the long wavelength transitions in unsubstituted carbohydrates were transitions of nonbonding electrons on oxygen containing groups (54, 55, 56). Within the spectral region here investigated, spectral contributions are limited to the following chromophores: hydroxyl, hydroxymethyl, the anomeric hydroxyl, the glucosidic, and the ring oxygen.

The wavelength of a chromophore is a function of its electronic properties. In solution, the bonding or intrusion of the solvent may perturb the ground and excited state energies of a chromophore and thereby determine its spectral location.

Prior work (55) on the anomers of glucose and of methyl-glucoside tentatively identified the first band to be the ring oxygen. The second band for methyl glucoside was assigned as the glycosidyl group. The short wavelength band, lying beyond 1700 Å, was assigned transitions including hydroxyl, hydroxymethyl, and anomeric hydroxyl groups.

An assignment of these chromophores to the two bands of amylose and of the glucose oligosaccharides will be based upon an understanding of solvent and intramolecular interactions relative to

the monomeric chromophores. Solvent interactions are determined by the configuration and geometry of groups neighboring the chromophore and by the solvent structure.

Table I lists the reported band positions of several carbohydrate ethers (54, 55, 56). It is seen that the ethers of α-glucose, α-methyl glucoside, and an α-glucose homomorph, xylose, each shift to longer wavelengths with increasing bulkiness of neighbor groups. It is thought that steric hinderance by neighboring groups blocks out solvent hydrogen bonding (54).

Table I. Assignment of chromophores.

| Chromophore | Configuration | Band Maximum |
|---|---|---|
| 1) Anomeric ether oxygen from α-methyl glucoside | 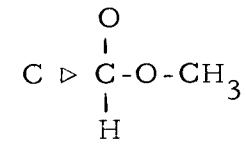 | 1720 Å |
| 2) Ring ether oxygen from xylose | 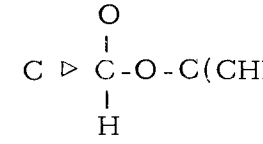 | unknown, but > 1810 Å |
| 3) Ring ether oxygen from α-methyl glucoside | 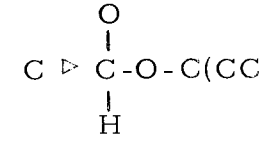 | 1810 Å |
| 4) Ring ether oxygen from α-glucose | identical to above | ~1810 Å |
| 5) Ring ether oxygen from α-1-4 glucans | identical to above | 1820-1850 Å (here assigned) |
| 6) Glucosidyl linkage oxygen from α-1-4 glucans | identical to above | 1820-1850 Å (here assigned) |

Also it is shown in Table I that, except for the ring ether on the reducing end, all ethers in α-1-4 glucans have identical configurations. If one assumes that identical configuration will result in identical or near identical solvent interaction, then solvent perturbation of the configurationally identical ether chromophores should be identical. The assignments of the long wavelength band are made on this assumption. The long wavelength band of the α-1-4 glucans is assigned to both the glucosidyl linkage ethers and the ring ethers (excluding the reducing end ring ether).

The assumption that identical configuration results in identical solvent interaction is in part verified by the work of Painter (57). In a study of the anomeric effect of maltose, Painter has shown that the ring ethers and glucosidyl linkage ether are indeed hydrogen bonded by the solvent water. We also know that hydrogen bonding of these ethers can be increased by the removal of steric hinderance (Table I). However, an ether can have at most two hydrogen bonds. Thus the number of hydrogen bonds of the glucosidyl linkage ether and glucosyl ring ether of identical configuration must be greater than zero but less than two.

As stated earlier, the hydroxyl, hydroxymethyl, and anomeric hydroxyl chromophores of glucose and α-methyl glucoside have been assigned to the short wavelength band, lying beyond 1700 Å (55). In the vapor phase, the hydroxyl band lies at 1820 Å (58). Since it is

reasonable to assume that glucan hydroxyls in aqueous solution participate in some type of hydrogen bonding, their spectral location must lie somewhere in the blue of 1820 Å.

Thus, as in the glucose monomer, the short wavelength band for the glucan is assigned to include the hydroxyl, the hydroxymethyl, and anomeric hydroxyl. In addition, transitions on the ethers are not confined to the long wavelength band, but probably also appear in the short wavelength band.

## Conformational Dependence on Circular Dichroism

The power of circular dichroism lies in its ability to distinguish chemical species which are chromophorically identical but conformationally different. The rotational strength of a transition, a measure of the circular dichroism, is entirely dependent upon the asymmetry of its environment. This is in contrast to the dipole strength, a measure of absorption, which to a first approximation is entirely independent of asymmetry in its environment. A study of the circular dichroism of a series of chromophorically related compounds should reveal conformational relationships among the series. This is such a study of amylose and the maltose oligomers.

Figures 14, 15, and 16 illustrate the conformational dependence of the circular dichroism of glucans. Figure 14 compares the observed maltose spectrum with an appropriate sum of the

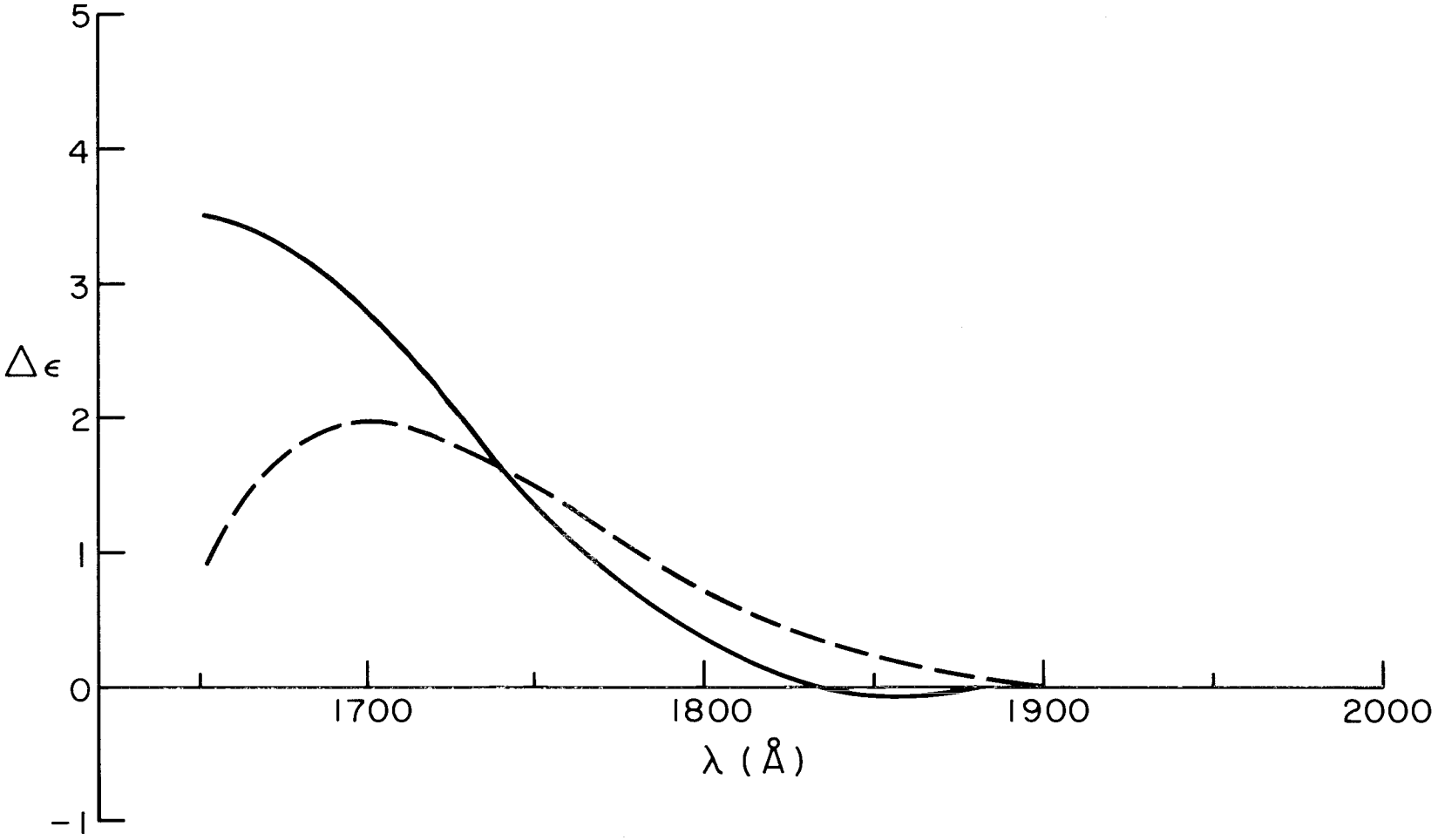


Figure 14. Comparison of the circular dichroism spectrum observed for maltose (——) and a circular dichroism spectrum constructed from an appropriate sum of the monomers (---): 50% α-methyl glucoside, 21.5% α-glucose, and 28.5% β-glucose.

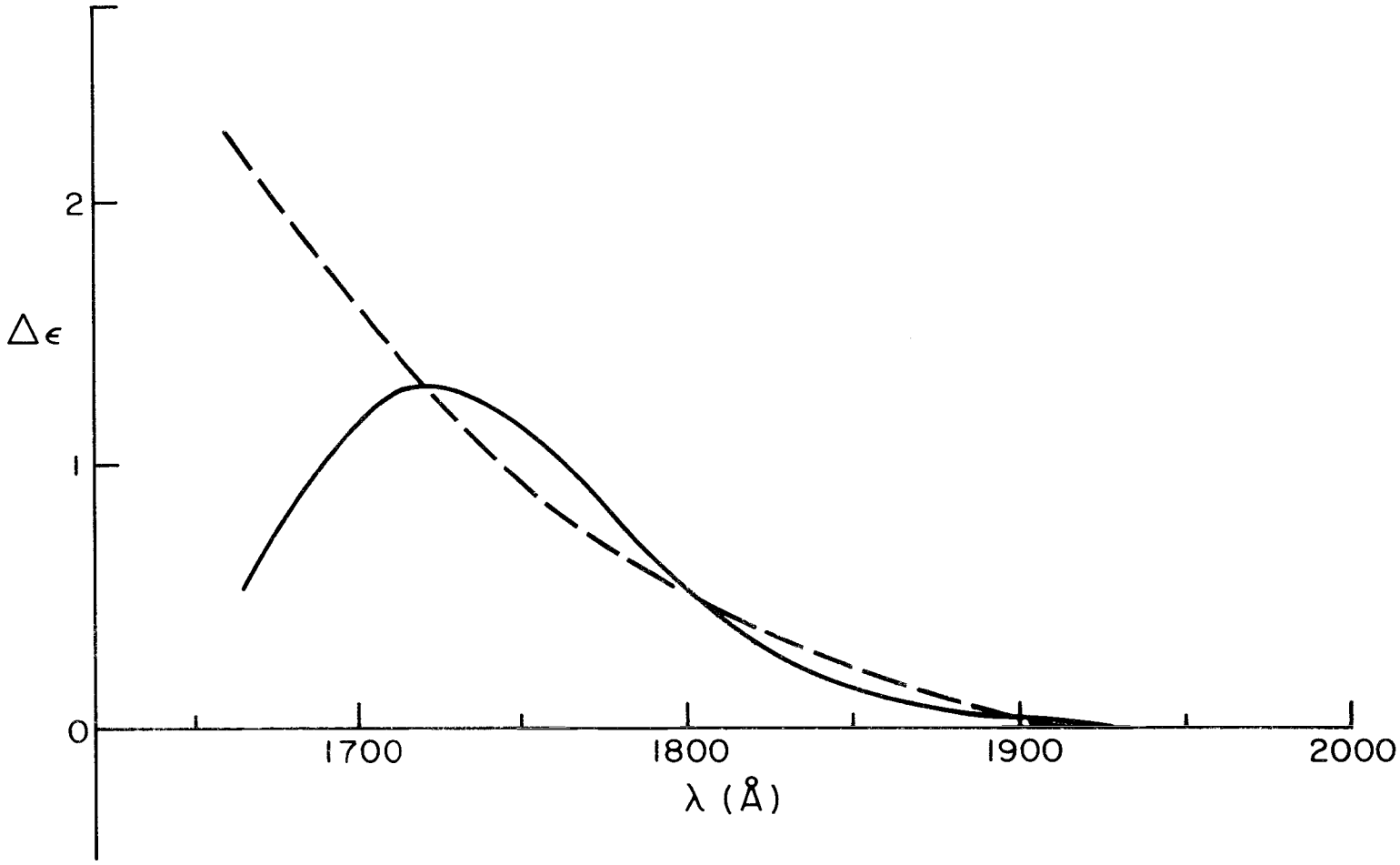


Figure 15. Comparison of the circular dichroism spectrum observed for cellobiose (——) and a circular dichroism spectrum constructed from an appropriate sum of the monomers (---): 50% β-methyl glucoside, 18% α-glucose, and 32% β-glucose.

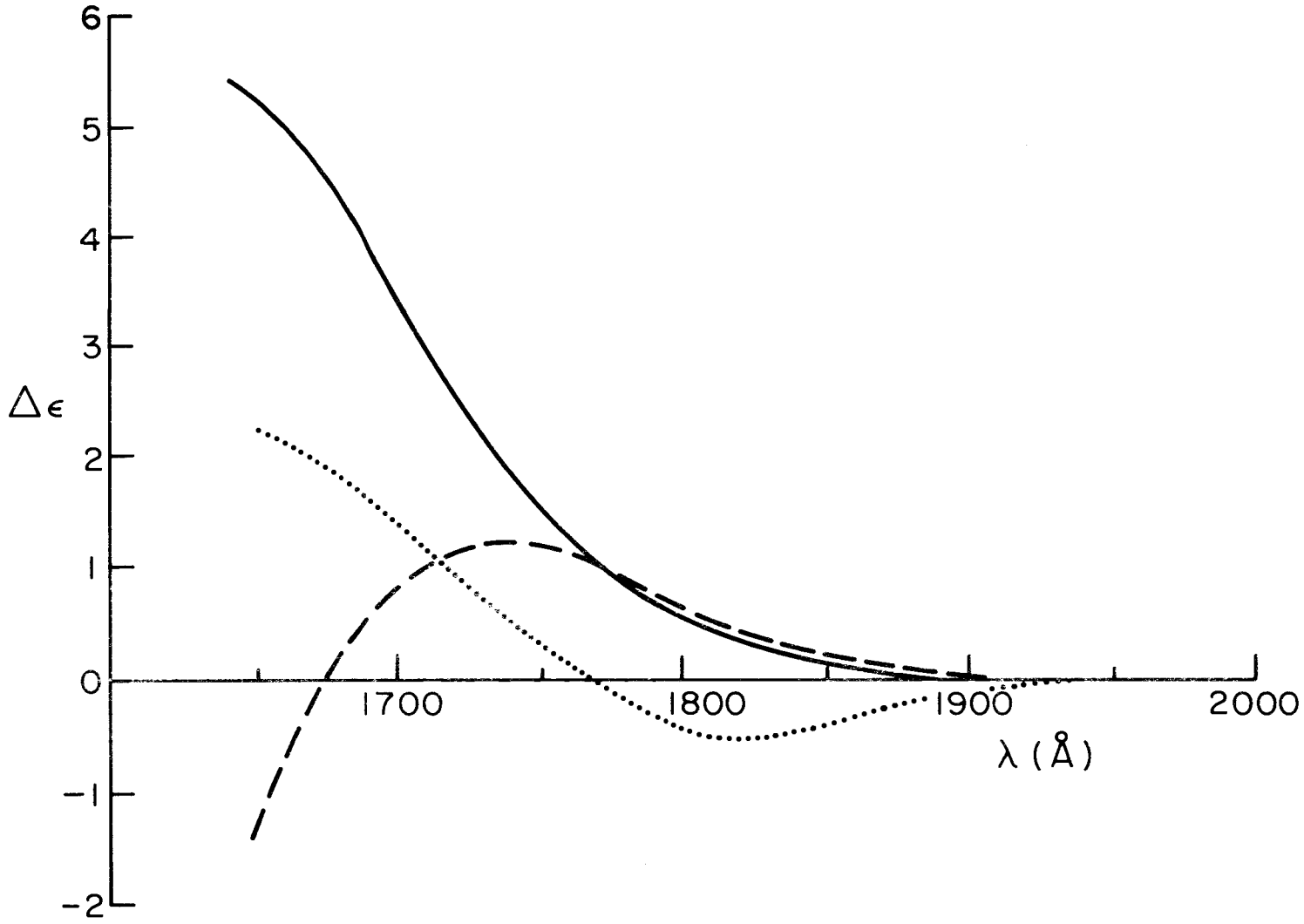


Figure 16. Comparison of the circular dichroism spectrum observed for amylose (· · · ·), for cyclohexylamylose (——), and for α-methyl glucoside (- - - -).

monosaccharide spectra: α-methyl glucoside (50%) and the glucose monomers (21.5% α and 28.5% β) (61). Alpha-methyl glucoside was chosen because it has a methoxy group of the correct anomeric configuration to represent the linkage oxygen in maltose. However, the glucose monomers contain an extra hydroxyl group at C-4 which is lost on forming this linkage. While this is a weak point in the comparison, we can see from Figure 15 that it does not affect our conclusions. Here we compare the observed cellobiose spectra with a sum of the monosaccharide spectra: β-methyl glucoside (50%) and the glucose monomers (18% α and 32% β) (61) chosen in a similar manner. In this comparison, the glucose monomers also have an extra hydroxyl group at C-4. However, the difference between the measured and monomer spectra is negative above 1700 Å where the hydroxyl absorbs while this difference was positive for maltose. This indicates that the C-4 hydroxyl is not a significant factor in the difference in circular dichroism between dimer and monomers. Indeed, these comparisons show that the circular dichroism of the monomers is significantly altered when incorporated into the dimer and perturbed by its neighbor. We would expect these perturbations to be related to the conformation about the linkage oxygen.

Figure 16 compares the spectra of amylose, cycloamylose, and α-methyl glucoside. Amylose and cyclohexylamylose are chromophorically identical. The cyclohexylamylose is clearly composed

entirely of interior glucosyl units. The contribution of the terminal group chromophores of amylose is negligibly small compared to the rest of the molecule so that amylose may be considered to be composed entirely of interior glucosyl units. The α-methyl glucoside is the monomer which corresponds to the interior glucosyl units. Although all three circular dichroism spectra are of interior glucosyl units, still all three circular dichroism spectra are very different. We attribute these differences to differences in conformation. Being cyclic, the conformation of the cyclohexylamylose is necessarily restricted. On the other hand, the conformation of free aqueous amylose is uncertain, but the circular dichroism spectra indicate that it is different from cyclohexylamylose. This illustrates the power of circular dichroism to distinguish among chromophorically identical but conformationally different species.

For a given solvent, it is useful to think of the conformation of glucans to be a function of only three independent variables: the glucosidyl linkage angle and the glucosyl rotational angles $\phi$ and $\psi$. Thus the linkage ether has three independent variables which determine the conformation of the entire glucan:

1. The bridge angle C(1)-O(1)-C(4') is found to vary between 113° and 119° in the solid state. For the maltose unit it is thought to average 117° (50). Increased temperature broadens the distribution of the angle value.

2. The glucosyl rotational angles about the C(1)-O(1), $\phi$,
3. and O(1)-C(4') bonds, $\psi$, are defined to be zero when O(4), C(4), C(1), O(1) and C(4'), C(1'), O(1') all lie in the same plane with the glucosyl units syndiotactically related (Figure 1). One calculation puts 90% of the partition function within 1.1% of the $\phi\psi$ conformational space (49).

Each glucosyl group in the glucans is thought to be in the C1 chair conformation (37, 62, 63, 64, 65). For a given chain geometry, the hydroxyl and hydroxymethyl orientation and hydrogen bonding will assume distributions to minimize their energy. They can therefore be considered dependent upon the chain geometry. The glucosyl rotational angles $\phi$ and $\psi$ and the glucosidyl linkage angle determines the overall conformation of the $\alpha$-1-4 glucans. All possible intramolecular interactions in the glucans are dependent on the linkage ether conformation. Small differences in the linkage ether conformation can cause large differences in the conformation of the glucan.

The circular dichroism of glucans is markedly dependent upon conformation. Since the three independent variables of the linkage oxygen determine the conformation, the glucosyl orientation about the linkage oxygen must also markedly affect the circular dichroism of glucans.

The conformational interrelationships developed in this study are entirely empirical. In an empirical investigation, the best

results are found from comparisons of the circular dichroism of compounds of known and unknown conformation. Like circular dichroism implies like conformation; unlike circular dichroism implies unlike conformation. A limiting factor in such studies is the availability of compounds of known conformation. It is anticipated that with improvements in the art of circular dichroism calculations based on quantum mechanics, this limitation can be side stepped and more information will result.

Evidence for Chirality Bias

The effect of chirality bias is indicated by a comparison of the circular dichroism spectra of amylose (Figure 3) and of the cyclodextrins (Figures 10 and 11). The sign of the ether band (long wavelength band) for each of these cyclic dextrins is positive. The sign of the ether band of amylose is negative. The intensity of the hydroxyl band (short wavelength band) is much greater for the cyclic dextrins than for amylose. Since the chromophores of amylose and the cyclodextrins are structurally equivalent, the differences in their spectra must be attributed to conformational differences.

Both cyclohexylamylose and cycloheptylamylose are pseudo helices with the average values of the conformational variables fixed because they are cyclic. Each has zero pitch, thus no chirality. Amylose, on the other hand, is believed to have a secondary structure

similar to these dextrins but helical. One might expect the conformation of amylose to be chiral in analogy to the chirality imposed upon nucleic acids by the sugar backbone. The difference in circular dichroism between the cyclodextrins and amylose demonstrates the chirality bias in amylose. If there were no chirality bias, the circular dichroism would resemble that of the dextrins. Since the differences of the circular dichroism of the cycloamyloses and amylose are substantial, the chirality bias should also be substantial.

The existence and direction of the helical sense of amylose has been in controversy (45, 49). The existence of a chirality bias in amylose is now indicated experimentally. However, the direction of the chirality bias has not yet been experimentally established. Verification of the calculated bias directions of amylose must await further experimental evidence.

Evidence for Helical Content

An inspection of the circular dichroism spectra of aqueous amylose and of amylose complexed with butanol in Figure 3 and 4 shows that there is little difference between the spectra. This marginal change in the circular dichroism spectra of amylose upon complexation with butanol is consistent with the putative conformational change and the power of circular dichroism to detect that

change. The amylose butanol complex has a V form helix conformation with the butanol complexed in the channel of the helix (52). The viscosity measurements discussed in the experimental section indicate that approximately 50% of the amylose is complexed with butanol for the circular dichroism presented in Figure 4. On the other hand, free aqueous amylose is believed to form loose extended helical regions which are interrupted by short disordered regions (22, 23, 25). The change of the conformation of the maltosyl subunits of amylose upon complexation with butanol should be very slight.

The conformational similarity of the maltosyl subunits of free amylose and the V form butanol complex is in agreement with several calculations on this subject (36, 44, 46, 47, 48, 49, 50). The V form butanol complex of amylose is thought to lie on a point in the occupied conformational space of uncomplexed amylose. Thus, the collapse of the occupied region to a point within that region upon complexation represents a small conformational change of the maltosyl subunits of amylose. Since molecular conformation determines the circular dichroism, the relative consistancy of the circular dichroism of amylose upon complexation with butanol indicates that the conformation of the maltosyl subunits of amylose has changed little.

Amylose and the Maltose Oligomers

In general, spectra of homopolymers may be treated as a sum of contributions from the two terminal units and from the interior polymer subunits. Of interest for any given polymer is the minimum number of subunits which comprise a terminal unit. This minimum number of subunits for the terminal unit is dependent upon the efficacy of subunit interaction at the interior terminal interface. The minimum number may also be dependent on conformational differences between the terminal units and the interior subunits. Thus given a low efficacy of subunit interaction, but extensive conformational differences, the terminal units could still be large.

The circular dichroism spectra of amylose and the maltose oligomers are consistent with a model which assigns a single glucosyl unit to each terminus. Circular dichroism data for this series has been fitted to the equation

$$\Delta\epsilon(\lambda) = \{[A(\lambda)+A'(\lambda)]+B(\lambda)(n-2)\}/n = \frac{A(\lambda)+A'(\lambda)-2B(\lambda)}{n} + B(\lambda) \quad (1)$$

where "A" and "A'" are the spectral contributions of the single glucosyl units at each terminus; "B" is the spectral contribution of the interior glucosyl subunits; and "n-2" is the number of interior glucosyl subunits in the polymer. Figure 17 shows that, within the

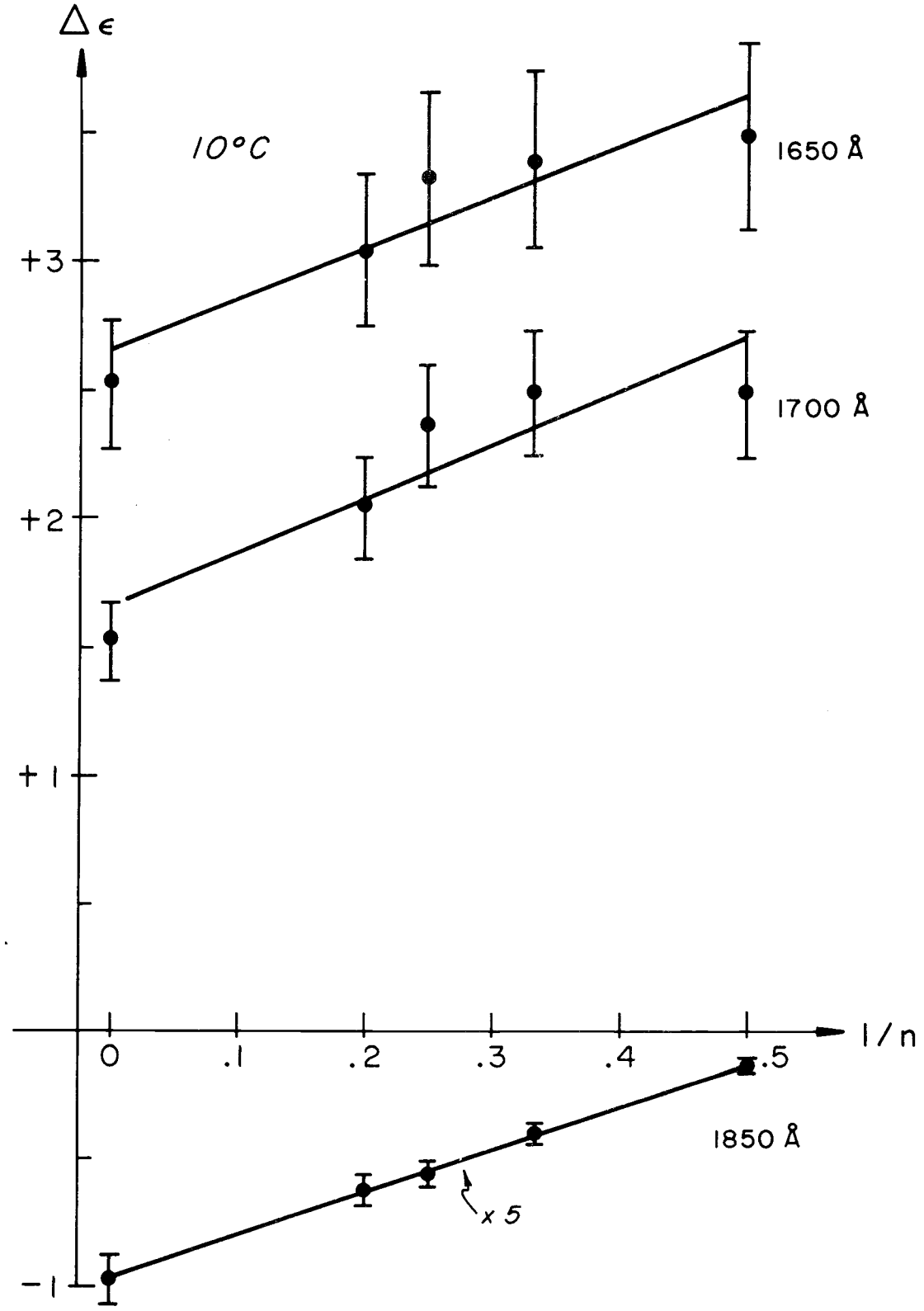


Figure 17. Circular dichroism of amylose and the maltose oligomers at three wavelengths (1650, 1700, 1850 Å) at 10°C plotted versus the reciprocal of the degree of polymerization. The error of the measurement is indicated by bars. The lines represent the least squares fit. The data is consistent with a simple homopolymer model.

experimental error, $\Delta\epsilon$ at three wavelengths is linearly related to the reciprocal of the degree of polymerization ("n") as predicted by Equation 1. Also Figure 18 shows that this relationship remains linear as the temperature changes between 10°C and 50°C. However, the slope and intercept may change with temperature. This agreement with Equation 1 shows that a single glucosyl unit satisfies the requirements of a terminal unit.

The implications for the fact that a single glucosyl subunit satisfies the requirements of a terminal unit for amylose and the maltose oligomer series are two fold:

1. Subunit interaction beyond the nearest neighbor do not materially affect the circular dichroism of this homopolymer.
2. The conformation of the interior subunits of maltotriose and higher oligomers approximates the conformation of the subunits of amylose. This means that the glucosyl ring conformation, the C(6) hydroxymethyl group orientation, and the glucosyl linkage of interior maltosyl units are all approximately equivalent for amylose and the maltose oligomer series.

It was a major disappointment that subunits interactions beyond the nearest neighbor did not materially affect the circular dichroism of amylose and the maltose oligomers. The literature on amylose is replete with reports on the importance of hydrogen bonding schemes

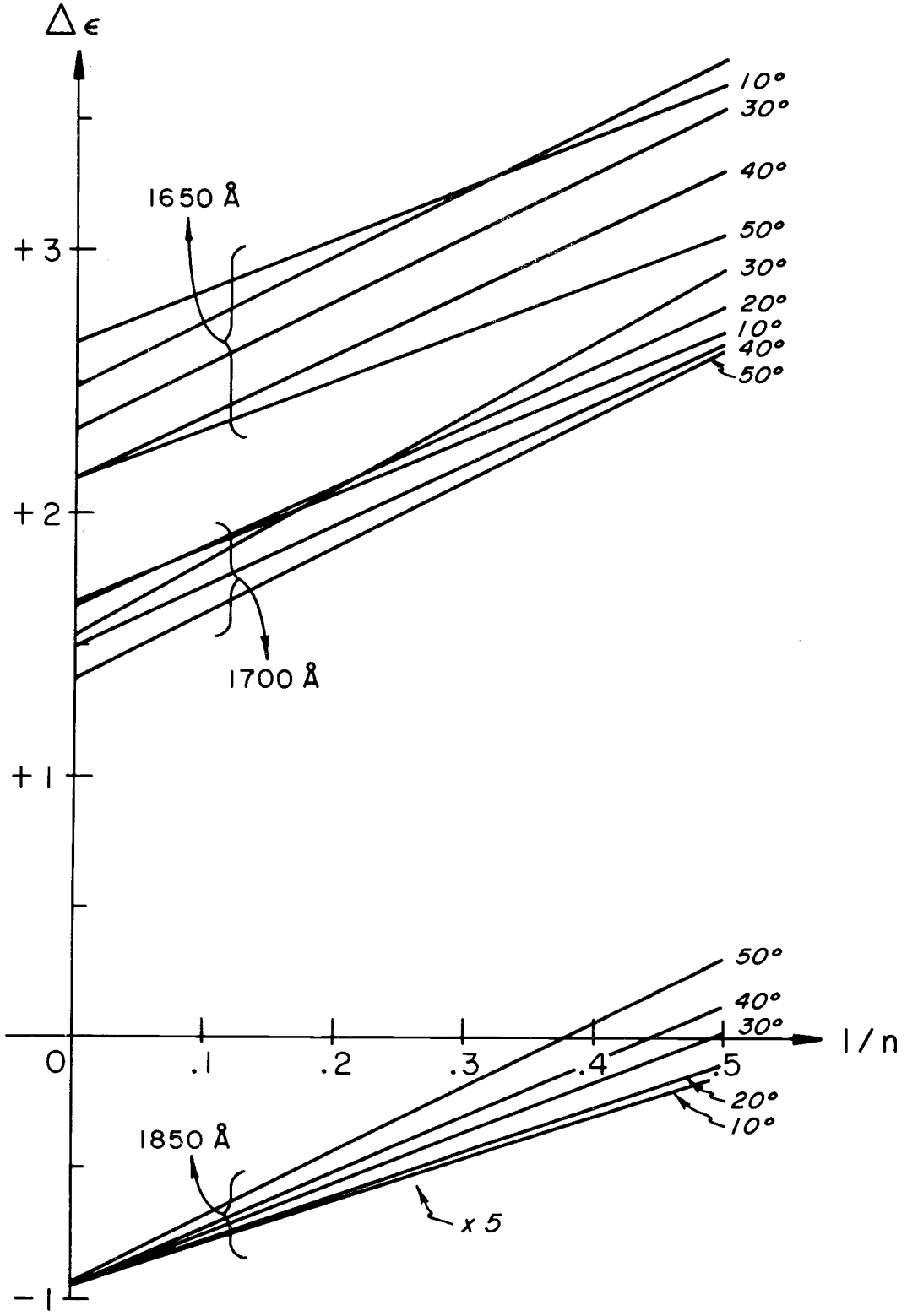


Figure 18. Same as Figure 17, except data is presented at five temperatures, 10, 20, 30, 40, and 50°C.

between groups on neighboring and distant glucosyl subunits which support helical structure (e.g., 38, 45, 49). At the out set of this investigation, it was hoped to find supportive evidence for these schemes. The inability of subunit interactions beyond the nearest neighbors to effect materially the circular dichroism of this homopolymer series, however, has precluded the possibility of such findings. Either the hydrogen bonding which hypothetically supports an ordered structure for amylose in solution does not exist or its effects on the circular dichroism to 1650 Å is so small as to be lost within the error of our measurements.

The circular dichroism spectra of amylose and the maltose oligomers is then an independent sum of contributions from terminal glucosyl units and interior glucosyl subunits. The two terminal units are chromophorically distinguishable from each other and from the interior glucosyls. The interior glucosyls are all chromophorically equivalent. The nonreducing terminal glucosyl is distinguished from the interior glucosyl only by a C(4) ether substitutuion. On the other hand, the reducing terminal glucose has a hemiacetal group while the interior glucosyls and nonreducing terminal glucosyl have acetal groups. The glucose monosaccharides experience a blue shift in the short wavelength band on changing from the hemiacetal to the acetal (see Figures 12 and 13). This same blue shift in the short wavelength band is seen in the amylose spectrum which corresponds to the

interior glucosyls of the "B" term when compared to the maltose spectrum which corresponds to the "A + A'" term of Equation 1. Thus the blue shift of the short wavelength band with increasing chain length of the maltose oligomers represents the declining relative importance of the hemiacetal group of the reducing terminus and ascending dominance of the interior acetal groups.

Temperature Effects--Evidence of a Loose Extended Helix

Phenomenologically, an increase in temperature has three effects common to the circular dichroism spectra of the glucans: (1) decrease of intensity, (2) red shift, and (3) formation of isosbestic points. Also, the relative temperature insensitivity of the circular dichroism of amylose indicates that the occupied conformational space of amylose includes a small region about the V form helix. This will result in a loose extended helix conformation for free amylose.

The low temperature sensitivity of amylose indicates that the occupied conformational space of amylose includes a small region about the V form helix point. From the circular dichroism spectrum of the butanol complex of amylose, it was shown that the conformation of the maltosyl subunits of amylose approximates the V form. However, from the temperature insensitivity of the circular dichroism of amylose it is seen that the conformation of free amylose need not be

identically the V form. Heated amylose is precluded from having a helical conformation (19). However, both the high and low temperature forms of the maltosyl subunits of amylose must be approximately the same since the circular dichroism is sensitive to maltosyl conformation. Thus the low temperature conformation of the maltosyl subunits need not be identically V form. This is consistent with a model for amylose which forms a loose extended helix.

The decreased intensity of circular dichroism band is frequently a measure of increased rotomeric activity (59). The broadening of the rotomeric density distribution will redistribute commensurately the contribution to optical activity of the rotomeric positions. In theory and in practice this generally has a depressing effect on the intensity of a band.

For the short wavelength band of the 1-4 glucans, the decreased intensity with increasing temperature has an obvious interpretation. Since the hydroxyl chromophores are themselves rotomers, the increased rotomeric activity of these chromophores would usually cause a decrease of their own band intensity. Second, the perturbation of the hydroxyl chromophores by other rotomeric groups would usually be such as to decrease the induced optical activity with increasing rotomeric activity, i.e., increased movement usually reduces the overall asymmetry of the chromophoric environment.

Other workers (15, 16) have found that the far ultraviolet optical rotatory dispersion spectra for amylose is positive and declines in intensity with increasing temperature. Our measurements corroborate these observations. The magnitude and temperature sensitivity of the optical rotatory power of amylose in the ultraviolet is dominated by the short wavelength band because of its greater magnitude. Optical rotatory power in the ultraviolet is relatively insensitive to the long wavelength ether band of amylose because of its relatively smaller size.

The red shifting of the bands with increased temperature indicates a decline in the efficacy of solvent interactions with the chromophores. This confirms that solvent interaction greatly influences the spectral energy of the transition of glucans.

The general case of isosbestic points generated by variation of temperature is described by Morrey (60). Isosbestic points generated by temperature variation are to be distinguished from constant temperature isosbestic points. Constant temperature isosbestic points are generated by variation of two and only two spectrophotometrically distinguishable species of mutually dependent concentration. The sum concentration of the two species remains constant, yielding isosbestic points at wavelengths of equal extinction ($\Delta\epsilon$) coefficients. On the other hand, Morrey has developed rules for the temperature generated isosbestic points which differ from the constant temperature case. By

argumentation involving the algebra of observed band transformations with temperature and by experimental demonstration, Morrey has found that in the general case temperature generated isosbestic points are indicative of the following (60):

1. One and only one species contributes to the absorbance ($\Delta\epsilon$) at a given isosbestic point.
2. The equilibrium of this species is not appreciably affected by temperature changes.
3. The absorbance ($\Delta\epsilon$) of a species at a given wavelength is linearly dependent on temperature to a good approximation.
4. Correction for liquid expansion does not destroy isosbestic points but may shift them.

Morrey's findings on isosbestic points are both necessary and sufficient. The certainty, however, of his findings increases with the size of the spectral region or the density of its isosbestic points. The absence of isosbestic points over a sufficiently large spectral region is indicative of the violation of one or more of Morrey's findings.

An application of Morrey's rules on isosbestic points to the circular dichroism spectra of glucans tells us that there is one and only one species present and that this species changes little in its equilibrium over the temperature range of 10° to 50°C for the following compounds: amylose, maltopentaose, maltotetraose, maltotriose, cycloheptylamylose, and cellobiose.

On the other hand, the absence or violation of anticipated isosbestic points indicates one of three alternatives: 1) That there are more than one species present; or 2) The species changes equilibrium significantly over the temperature range of 10° to 50°C; or 3) The circular dichroism at each wavelength is not linearly dependent on temperature. One or more of these alternatives applies to the following compounds: amylose in aqueous butanol, maltose, and cyclohexylamylose. This is consistent with and corroborative of but not conclusive of: 1) The two state model for complexed amylose as advanced by Hamori (22, 23, 25). 2) The importance of the end effect for maltose, i.e., varying population of $\alpha$ and $\beta$ anomers (61). 3) The high sensitivity of the conformation of cyclohexylamylose to the water activity in its hydrophobic cavity (41).

# CONCLUSIONS AND SUMMARY

The circular dichroism of several 1-4 glucans was measured at different temperatures in the vacuum ultraviolet to 1640 Å. The α-1-4 glucans had two bands in this region. The short wavelength band was always positive and much larger than the long wavelength band. The long wavelength band was negative for the linear α-1-4 glucans and positive for the cyclodextrins.

The first band is assigned to transitions on the ring and linkage ethers by analogy with the monomer assignments and by the argument that solvent hydrogen bonding greatly affects the energy of these transitions. Equivalent configuration was assumed to result in equal or near equal solvent interaction. The second band, the short wavelength band, is assigned to the various hydroxyls and to further transitions on the ethers for similar reasoning.

The circular dichroism of glucans is shown to be sensitive to conformation. A comparison of the circular dichroism of maltose and cellobiose with spectra constructed from an appropriate combination of the monomers illustrates that the interaction between neighboring glucosyl units significantly affects the circular dichroism. A comparison of the circular dichroism of amylose, cycloamylose, and α-methyl glucose illustrates that the circular dichroism of glucans

is markedly sensitive to the relative orientation of neighboring glucosyl units.

The circular dichroism spectra of amylose and the maltose oligomers are in agreement with a homopolymer model which has terminal units of one glucosyl unit in length and intervening interior glucosyl units which are spectroscopically equivalent. The homopolymer model accurately accounts for the circular dichroism data for this series. This shows that all interior maltosyl units are equivalent in conformation for amylose and the maltose oligomers. Subunit interaction beyond the nearest neighbor does not materially effect the circular dichroism of this homopolymer.

Because the spectral contributions of interior groups of amylose differ from the cycloamyloses, the spectra must reflect a substantial chirality bias for amylose. Since the conformation of interior maltosyl subunits is identical for amylose and the maltose oligomers, the same chirality bias must also occur in the maltose oligomers. This chirality bias has been predicted but has not been experimentally observed before.

The similarity of the circular dichroism spectra of aqueous amylose and the amylose-butanol complex indicates that the conformational change of the maltosyl subunits of amylose upon complexation is small. This had been predicted by several calculations.

Also since the conformation of the maltosyl subunits of amylose in aqueous solution and in the butanol complex are approximately the same and since the conformation of the interior maltosyl subunits of amylose and the maltose oligomers is approximately identical, the conformation of the maltosyl subunits in the amylose-butanol complex and the maltose oligomers must also be approximately identical.

The low temperature sensitivity of amylose is consistent with a model for amylose in which the occupied conformational space is a small region which includes the V form helix point. A comparison of the circular dichroism spectra of amylose and the amylose butanol complex indicated that the conformation of the maltosyl subunits of free amylose approximates and may include the V form helix. However, since heated amylose is precluded from having a helical structure (19), and since the low temperature sensitivity of amylose indicates that the conformation of the maltosyl subunits of amylose changes little with temperature, the conformation of the maltosyl subunits of amylose need not be identically V form. This is consistent with a model for amylose which forms a loose extended helix.

The negative temperature sensitivity of both bands is interpreted as caused by increased rotomeric activity with increased temperature. The spectral red shift with increased temperature was attributed to decreased solvent hydrogen bonding.

The presence of temperature generated isosbestic points in the spectra of amylose, maltopentaose, maltotetraose, maltotriose, cycloheptylamylose and cellobiose shows that these compounds have one and only one spectroscopically distinguishable species and that the equilibrium of this species is not appreciably effected by temperature between 10° and 50°C. The absence of anticipated temperature generated isosbestic points in the amylose butanol complex, maltose, and cyclohexylamylose is supportive but not conclusive of two state or multiple state models for these systems.

In summation, the interior maltosyl subunits of free aqueous amylose and of the maltose oligomers series form a loose extended helix approximately equivalent to the V form helix. The conformation of all these species contain a substantial and approximately identical chirality bias. This data is consistent with a model for these species in which the occupied conformational space includes the V form helix point and a region about it.

Future work in this field should include circular dichroism studies on the conformation of the branched components of starch and of interactions between the branched and the linear components. Also, circular dichroism studies should be made on amylose and the branched components complexed to a number of compounds. Recently some 45 of these complex forming compounds have been catalogued and studied (26). These complexes are thought to form 6, 7 and 8

fold helices. Also circular dichroism studies can be made on x-ray characterized films.

Previous workers have studied the ORD of amorphous amylose films and of both V and B helical form films characterized by x-ray (13). The circular dichroism of films of differing combinations of interacting starch components would also be interesting to study. Finally, it would be of interest to identify the presence and role of complexing compounds within the developing or germinating potato.

# BIBLIOGRAPHY


1. Cato, Marcus Pocius. De Agri Cultura (De Re Rustica), S.S. 87, 149 B.C.

2. Banks, W., C.T. Greenwood, and D.D. Muir. Studies on the biosynthesis of starch granules. Part 6. Properties of the starch granules of normal barley and barley with starch of high amylose content during growth. Staerke 25(7):225-256 (July 1973).

3. Duffus, C.M. and R. Rosie. Purification and Fractionation of Potato Amyloplasts. Analytical Biochemistry 65(1):11-18 (1975).

4. Mercier, Christiane. The fine structure of corn starches of various amylose-percentage: Waxy, normal, and amylomaize. Staerke 25(3):78-83 (1973).

5. Banks, W., C.T. Greenwood, and D.D. Muir. Studies on the biosynthesis of starch granules. Part 5. Properties of the starch components of normal barley; and barley with starch of high amylose-content during growth. Staerke 25(5):153-188 (April 1973).

6. Yamashita, Yuhiko and Kuzuo Monobe. Single crystals of amylose V complexes. III. Crystals with $8_1$ helical configuration. Journal of Polymer Science (A-2):1471-1481 (1971).

7. Gruber, Von E., K. John, and J. Schurz. Versuche zur guellung des kartoffelstaerkekorns. Staerke 25(4):109-152 (April 1973).

8. Pfannemuller, B., H. Mayerhofer, and R.C. Schulz. Conformation of amylose in aqueous solutions: Optical rotatory dispersion and circular dichroism of amylose-iodine complexes and dependence on chain length of retrogradation of amylose. Biopolymers 10(2):243-261 (1971).

9. Johnson, J.A. and R. Srisuthep. Physical and Chemical Properties of Oligosaccharides. Cerial Chemistry 52(1):70-78 (1975).

10. Manners, D.J. and J.R. Stark. $\alpha$-(1 $\rightarrow$ 4)-D-Glucans. Part XXII. The iodine staining properties of linear maltosaccharides. Staerke 26(3):78-80 (1974).

11. McMullan, R.K., W. Saenger, J. Fayos, and D. Mootz. Topography of cyclodextrin inclusion complexes. Part II. Carbohydrate Research 31(2):211-227 (June 1973).

12. Backwell, J., A. Sarko, and R.H. Marchessault. Chain conformation in B amylose. The Journal of Molecular Biology 42:379-383 (1969).

13. Beychok, Sherman and Elvin A. Kabat. Optical activity and conformation of carbohydrates. I. Optical rotatory dispersion studies on immunochemically reactive amino sugars and their glycosides, milk oligosaccharides, oligosaccharides of glucose, and blood group substances. Biochemistry 4(12):2565-2574 (December 1965).

14. Purvinas, R.M. and H.F. Zobel. Optical rotatory dispersion of amylose films. Carbohydrate Research 10:129-139 (May 1969).

15. Rao, V.S.R. and Joseph F. Foster. Studies of the conformation of amylose in solution. Biopolymers 1:527-544 (1963).

16. Kuge, Takashi and Sozaburo Ono. Physicochemical properties of dilute aqueous solutions of amylose. Optical rotatory, viscometric and osmometric studies. Bulletin of the Chemical Society of Japan 34(9):1264-1270 (September 1961).

17. Dintzis, F.R. and R. Tobin. Optical rotation of some α-1,4-linked glucopyranosides in the system $H_2O$-DMSO and solution conformation of amylose. Biopolymers 7(4):581-593 (1969).

18. Rees, D.A. Conformational analysis of polysaccharides. Part V. The characterization of linkage conformations (chain conformations) by optical rotation at a single wavelength. Evidence for distortion of cyclohexamylose in aqueous solution. Optical rotation and the amylose conformation. Journal of the Chemical Society Part B: Physical Organic, 1970, pp 877-884 (1970).

19. Szejtli, J., M. Richter, and S. Augustat. Molecular configuration of amylose and its complexes in aqueous solution. Part II. Relation between the D.P. of helical segments of the amylose-iodine complex and the equilibrium concentration of free iodine. Biopolymers 5:5-16 (1967).

20. Szejtli, J., S. Augustat, and M. Richter. Molecular configuration of amylose and its complexes in aqueous solutions. Part III. Investigation of the D.P. distribution of helical segments in amylose-iodine complexes. Biopolymers 5:17-26 (1967).

21. Szejtli, J., M. Richter, and S. Augustat. Molecular configuration of amylose and its complexes in aqueous solutions. Part IV. Determination of D.P. of amylose by measuring the concentration of free iodine in solution of amylose-iodine complex. Biopolymers 6:27 - 41 (1968).

22. Thompson, John Crafts. A kinetic study of the rapid reaction between amylose and iodine. Ph.D. Thesis. University of Deleware (1970).

23. Senior, Marilyn and Eugene Hamori. Investigation of the effect of amylose/iodine complexation on the conformation of amylose in aqueous solution. Biopolymers 12:65-78 (1973).

24. Hollo, Janos and Joysef Syeitli. The reaction of starch with iodine. Chapter 7 in Starch and Its Derivatives. Fourth Edition, J.A. Radly, ed. Chapman and Hall Ltd., London, 203 p. 1968.

25. Hamori, Eugene and Marilyn B. Senior. Kinetic and hydrodynamic studies relating to the structure of the amylose macromolecule in aqueous solution. Annals New York Academy of Sciences, 210, pp 34-38 (1973).

26. Hybl, Albert, Robert E. Rundle, and Donald E. Williams. The crystal and molecular structures of the cyclohexa-amylose-potassium acetate complex. Journal of the American Chemical Society 87(13):2779-2788 (July 6, 1965).

27. Banks, W., C.T. Greenwood, D.J. Hourston, and A.R. Procter. Amylose in aqueous solution - A viscometric study. Polymer 12(7):452-466 (1971).

28. Banks, W. and C.T. Greenwood. Viscosity and sedimentation studies on amylose in aqueous solution - Further evidence for non helical character. European Polymer Journal 5:649-648 (1969).

29. Banks, W. and C.T. Greenwood. On hydrogen bonding in amylose. Biopolymers 11:315-317 (1972).

30. Senior, Marilyn Bowman. Physical characterization of biopolymers. Ph.D. Thesis, University of Delaware (1973).

31. Nishida, K. Interaction of acridine orange and amylose in a binary liquid system, dimethyl sulphoxide water. Colloid and Polymer Science 252: 1001-1002 (1974).

32. Takeo, Ken'ichi and Takashi Kuge. Complexes of starchy materials with organic compounds. Part III. X-ray studies on amylose and cyclodextrin complexes. Agricultural and Biological Chemistry 33(8):1174-1180 (August 1969).

33. Takeo, K., A. Tokumura, and T. Kuge. Complexes of starch and its related materials with organic compounds. Part X. X-ray diffraction of amylose-fatty acid complexes. Staerke 25(11):357-358 (November 1973).

34. Hinkle, M.E. and H.F. Zobel. X-ray diffraction of oriented amylose fibers. III. The structure of amylose-n-butanol complexes. Biopolymers 6:1119-1128 (1968).

35. Zaslow, Bert, Vincent Gerard Murphy, and Alfred Dexter French. The V amylose-$H_2O$ system: Structural changes resulting from hydration. Biopolymers 13:779-790 (1974).

36. Cael, J.J., J.L. Koenig, and J. Backwell. Infrared and raman spectroscopy of carbohydrates. Carbohydrate Research 29(1): 123-134 (1973).

37. French, Alfred D. and Vincent G. Murphy. The effects of changes in ring geometry on computer models of amylose. Carbohydrate Research 27(2):391-406 (1973).

38. Sundararajan, P.R. and V.S.R. Rao. Studies on the helical conformational of amylose and possible interconversions. Biopolymers 8:313-323 (1969).

39. Koenig, J.L. and P.D. Vasko. Infrared studies of chain folding in polymers. VIII. Metastable conformations in amylose. Journal of Macromolecular Science. Part B: Physics, B4(2): 369-380 (June 1970).

40. Rundle, R.E. and Frank C. Edwards. The configuration of starch in the starch-iodine complex. IV. An x-ray diffraction investigation of butanol-precipitated amylose. Journal of the American Chemical Society 65:2200-2203 (November 1943).

41. Manor, Philip C. and Wolfram Saenger. Water molecule in hydrophobic surroundings: Structure of α cyclodextrin-hexahydrate $(C_6H_{10}O_5)_6 \cdot 6H_2O$. Nature 237:392-393 (June 16, 1972).

42. Chu, Shirley S.C. and G.A. Jeffrey. The refinement of the crystal structures of β-D-glucose and cellobiose. Acta Crystallographica B24:830-838 (June 15, 1968).

43. Chu, Shirley S.C. and G.A. Jeffrey. The crystal structure of methyl β-maltopyranoside. Acta Crystallographica 23(6):1038-1940 (December 10, 1967).

44. Quigley, G.J., A. Sarko, and R.H. Marchessault. Crystal and molecular structure of maltose monohydrate. Journal of the American Chemical Society 92(20):5834-5839 (October 7, 1970).

45. Sundaralingam, M. Some aspects of stereochemistry and hydrogen bonding of carbohydrate related to polysaccharide conformation. Biopolymers 6:189-213 (1968).

46. Rao, V.S.R., N. Yathindra, and P.R. Sundararajan. Configurational statistics of polysaccharide chains. Part I. Amylose. Biopolymers 8:325-333 (1969).

47. Rao, V.S.R., P.R. Sundararajan, C. Ramakrishnan, and G.N. Ramachandran. Conformational studies of amylose. In Conformation of Biopolymers. G.N. Ramachandran, ed. Academic Press, pp 721-838 (1967).

48. Goebel, Kenneth G. and David A. Brant. The configuration of amylose and its derivatives in aqueous solution. Experimental results. Macromolecules 3(5):634-643 (September-October 1970).

49. Goebel, Carol V., William L. Dimpfl, and David A. Brant. The conformational energy of maltose and amylose. Macromolecules 3(5):644-654 (September-October 1970).

50. Brant, David A. and William L. Dimpfl. A theoretical interpretation of the aqueous solution properties of amylose and its derivatives. Macromolecules 3(5):655-664 (September-October 1970).

51. Banks, W. and C.T. Greenwood. Physico-chemical studies on starches. Part XXXIV. The distribution of molecular weight in amylose samples obtained by leaching and the dispersion of potato starch. Carbohydrate Research 6:171-176 (1968).

52. Banks, W. and C.T. Greenwood. Amylose: A non-helical biopolymer in aqueous solution. Polymer 12(1):141-144 (January 1971).

53. Johnson, W.C. A circular dichroism spectrometer for the vacuum ultraviolet. Review of Scientific Instruments 42:1283 (1971).

54. Nelson, Richard G. and W. Curtis Johnson, Jr. Optical properties of sugars. III. Circular dichroism of individual anomers. (in preparation).

55. Nelson, Richard G. and W. Curtis Johnson, Jr. Optical properties of sugars. IV. Circular dichroism of the methyl-glycosides. (in preparation).

56. Dickinson, Helen R. and W. Curtis Johnson, Jr. Optical properties of sugars. II. Vacuum-ultraviolet absorption of model compounds. Journal of the American Chemical Society 96(16):5050 (August 7, 1974).

57. Painter, Terence. Influence of cosolutes upon the conformation of carbohydrates in aqueous solutions. II. Demonstration of the anomeric effect in cellobiose and maltose, and proposal of a mechanism for the influence of inorganic ions upon its magnitude. Acta Chemica Scandinavica 27:3839-3860 (1973).

58. Snyder, P.A. and Johnson, W.C. Circular dichroism of (t)-2-butanol in the vacuum ultraviolet. A comparison of theoretical and experimental values. Journal of Chemical Physics 59(5): 2618-2628 (1973).

59. Kauzmann, Walter and Henry Eyring. The effect of the rotation of groups about bonds on optical rotatory power. Journal of Chemical Physics 9:41-53 (1941).

60. Morrey, J. R. Fused salt spectrophotometry. III. Isosbestic points generated by variations in temperature. Journal of Physical Chemistry 66:2169-2173 (1962).

61. Usui, Taichi et al. Proton magnetic resonance spectra of D-gluco-oligosaccharides and D-glucans. Carbohydrate Research 33: 105-116 (1974).

62. Rao, V.S.R. and Joseph F. Foster. On the conformation of the D-glucopyranose ring in maltose and in higher polymers of D-glucose. Journal of Chemical Physics 67(4):951-952 (April 1963).

63. Glass, C.A. Proton magnetic resonance spectra of D-glucopyranose polymers. Canadian Journal of Chemistry 43(10):2652-2659 (October 1965).

64. Reeves, Richard E. Cuprammonium-glycoside complexes. Advances in Carbohydrate Chemistry 6:107-134 (1951).

65. Casu, B. and M. Reggiani. Infrared spectra of amylose and its oligomers. Journal of Polymer Science. Part C: Polymer Symposium 7:171-185 (1964).

66. Casu, B., M. Reggiani, G.G. Gallo, and A. Vigevani. Conformation of O-methylated amylose and cyclodextrins. Tetrahedron 24:803-821 (1968).

67. Casu, B., M. Reggiani, G.G. Gallo, and A. Vigevani. Conformation of acetylated cyclodextrins and amylose. Carbohydrate Research 12:157-170 (1970).

68. Casu, B., M. Reggiani, G.G. Gallo, and A. Vigevani. Hydrogen bonding and conformation of glucose and polyglucoses in dimethylsulphoxide solution. Tetrahedron 22(9):3061-3083 (1966).

# APPENDIX

# APPENDIX

Reprinted from Journal of Molecular Biology (1974) 86, 91-96

## Circular Dichroism of DNA in the Vacuum Ultraviolet

Donald G. Lewis and W. Curtis Johnson Jr.*

Department of Biochemistry and Biophysics

Oregon State University, Corvallis, Oregon 97331

*Recipient of Public Health Service Research Career Development Award No. GM 32784

## Summary

The circular dichroism spectrum of DNA in aqueous solutions is advanced far into the vacuum ultra violet region to about 164 nm. Both the native and heat denatured forms of DNA from calf thymus, Clostridium perfringens, Escherichia coli, Micrococcus lysodeikticus, and T-7 Bacteriophage are studied. Observed for the native form is a new band at about 168 nm. The vacuum ultra violet region of the spectrum is much more sensitive to the source of DNA than is the near ultra violet portion. In fact, the band at 188 nm which had previously been reported for calf thymus DNA only, is observed to be resolved into two peaks for Clostridium perfringens DNA. For the heat denatured form, two new bands at about 171 nm and 191 nm are reported for the first time. The vacuum ultra violet region of the spectrum is discovered to change much more strikingly upon heat denaturation than the near ultra violet. The extension of the circular dichroism spectrum results in new parameters which will aid in the precision of empirical correlations and theoretical calculations on the sequence and conformation of DNA.

## Introduction

The optical activity of DNA at the sodium D line was first measured by Jones (1908), forty years after the initial discovery of

nucleic acids by Freidrich Mischer. Because of the low sensitivity of the available polariscope, it was necessary to make the rotational measurements on low opacity DNA gelatins. These first measurements were not quantitative. Much later, Drude plots of visible ORD measurements on DNA solutions indicated that the first optically active absorption band should lie in the near ultra violet (Summarized in Fresco 1961a). Fresco and coworker (1961b) then verified this prediction by the attempted measurement on a modified polarimeter of the multiple Cotton effects of optically dense DNA solutions in the 250-300 nm region. This was soon followed by circular dichrograph measurements in the near ultra violet (Brahms & Mommaerts, 1964) The circular dichroism spectrum of DNA has since been measured in the far ultra violet (Sarkar 1967) and into the vacuum ultra violet (Li, et al., 1971). In this paper, we extend the spectrum far into the vacuum ultra violet to about 164 nm. This is the first systematic study of the optical activity of several DNA's in the vacuum ultraviolet.

Justification for measuring the optical activity of DNA lies in the fact that sequence and conformational information is reflected in these measurements. The work of Tunis-Schneider and Maestre (1971) on DNA films has supplied the connection between the well characterized solid state conformations of DNA and solution conformations. It is hoped that the new bands which we present here will

increase the sensitivity of circular dichroism measurements to this type of information.

Corroborating these measurements are a number of quantum mechanical calculations which relate the circular dichroism to the conformation of DNA. Future improvements on these calculations are anticipated. The increased number of circular dichroism bands presented in this paper can now be utilized for such calculations.

## Materials

Calf thymus DNA was purchased from Worthington Biochemicals, Inc. Protein content of the Worthington calf thymus DNA was measured by the Lowry method (Shatkin, 1969). All measurements fell around 2% protein by weight, depending on the lot number. Protein content was reduced to less than 1% by means of (1) a pronase digest; (2) six alternate extractions with water saturated phenol and with formaldehyde in the presence of 6 M NaF; and (3) an alcohol precipitation. There was no difference in the spectra between the treated and untreated DNA. It was calculated that, even if the protein were entirely in the α-helical form, then the greatest possible error due to 1% protein contamination would be less than 4% of the value of either DNA band in the vacuum ultraviolet.

T-7 phage DNA was obtained by three phenol extractions from phage purified by centrifugation on a CsCl gradient. The protein

content was checked by the 260/280 and 260/220 method. It was found to be protein free within the accuracy of this measurement.

The Clostridium perfringens and Escherichia coli DNA were purchased from Worthington Biochemicals, Inc. The Micrococcus lysodeikticus DNA was purchased from Sigma Biochemicals Co. All three bacterial DNA's were used without further purification. The protein content of each was approximately 1% as measured by the Lowry Method.

The DNA was dissolved in and dialyzed against aqueous solutions of $10^{-3}$ NaF. The fluoride ion was used because of its greater transparency in the vacuum ultraviolet compared to other anions. Since all buffering systems absorb light in the vacuum ultraviolet, the DNA was left unbuffered. However, at the high concentrations used some self buffering was observed giving a pH of 6.8. The salt concentration was chosen to be $10^{-3}$ in order that the DNA might denature at a relatively low temperature. The hyperchromicity of the spectrum at 60°C for each of the DNA's indicated that the melting transition temperature had been fully passed. It has been previously observed that the circular dichroism of DNA is an active function of the temperature (Gennis & Carter, 1972 and references therein). Therefore when we use the term "heat denatured" we mean that the DNA has suffered its major hyperchromic transition in absorbance.

## Methods

The spectral measurements were made on a vacuum ultra violet circular dichroism spectrophotometer described elsewhere (Johnson, 1971). The near ultra violet region was verified on a Durrum Jasco Model J-10 spectrophotometer. Very short pathlengths were used to minimize absorption by the water solvent in the vacuum ultra violet. For the shortest pathlengths, a droplet of DNA solution, 1% by weight, was pressed between two suprasil quartz discs. The pathlength using this method approached four microns. Under these conditions, linear dichroism can easily be produced. In fact to avoid linear dichroism we were required to reduce the viscosity by shearing the DNA by forcing it through a number 26 gauge syringe needle, and to use care in interposing the solution between the windows. We checked for linear dichroism in the well characterized near ultra violet region (see for instance, Wooley & Holzworth, 1971).

The concentration of the solutions were determined by adsorption at 258 nm assuming extinction coefficients taken from Felsenfeld and Hirschman (1965). The value of $\Delta OD$ was calculated by standardizing the output of the spectrophotometer against d-10-camphorsulfonic acid assuming a $\Delta\epsilon_{(290.5)}$ of 2.20. Since the highest energy peak was accessible only by the use of the shortest pathlength technique, its $\Delta OD$ was determined by a comparison with

the next highest energy peak which was measured in cells of known pathlength (65, 100 and 500 microns).

For all the spectra, the total OD (i.e. absorption and reflection by solvent, solute and windows) was kept less than one. The ratio of the intensity of stray light to unscattered light at 1630 A was measured to be less than one part in $10^5$.

To avoid air bubble formation in the sample during the 60°C scanning, the DNA solution was saturated with helium thus driving off the air. Helium, unlike air, has the property that it is more soluble in water at elevated temperatures than at lower temperatures. The use of $D_2O$ in the place of $H_2O$ allowed the spectrum to be extended about 20 Å further into the ultra violet. The spectra of DNA in $H_2O$ and $D_2O$ were superimposable within our error.

## Results and Discussion

The circular dichroism spectra of the five DNA's, native and denatured, are shown in Figures 1 through 5. The five DNA's which are studied represent a broad spread in base composition. The base composition of the five sources, given as the mole fraction of guanine and cytosine (G:C), are as follows (Marmur & Doty 1962): Clostridium perfringens, G:C = 0.31; calf thymus, G:C = 0.419; T-7 bacteriophage, G:C = 0.48; Escherichia coli, G:C = 0.501; and Micrococcus lysodeikticus, G:C = 0.719.

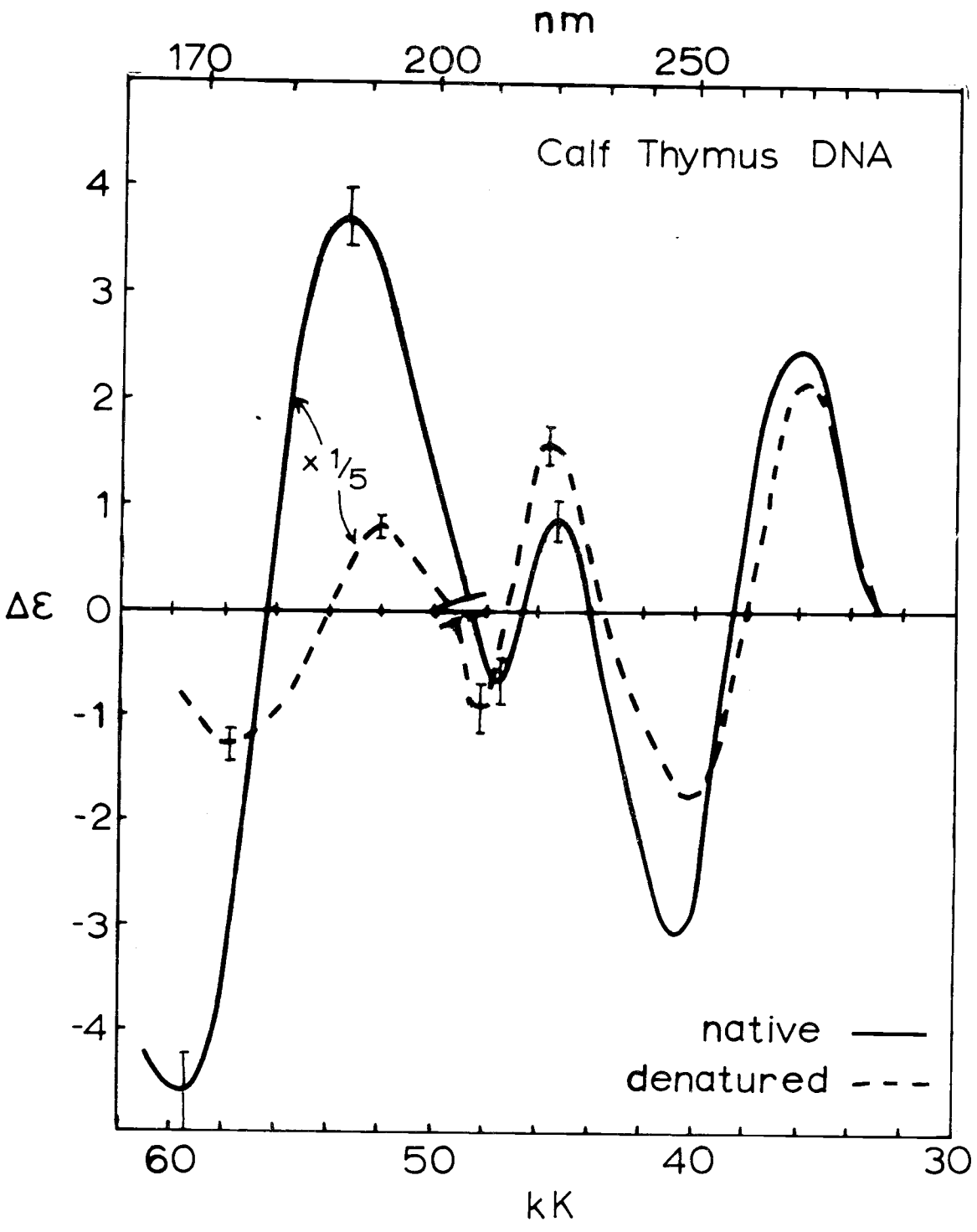


Figure 1. Measured circular dichroism for aqueous solutions of native (——) and heat denatured (- - -) calf thymus D. N. A.

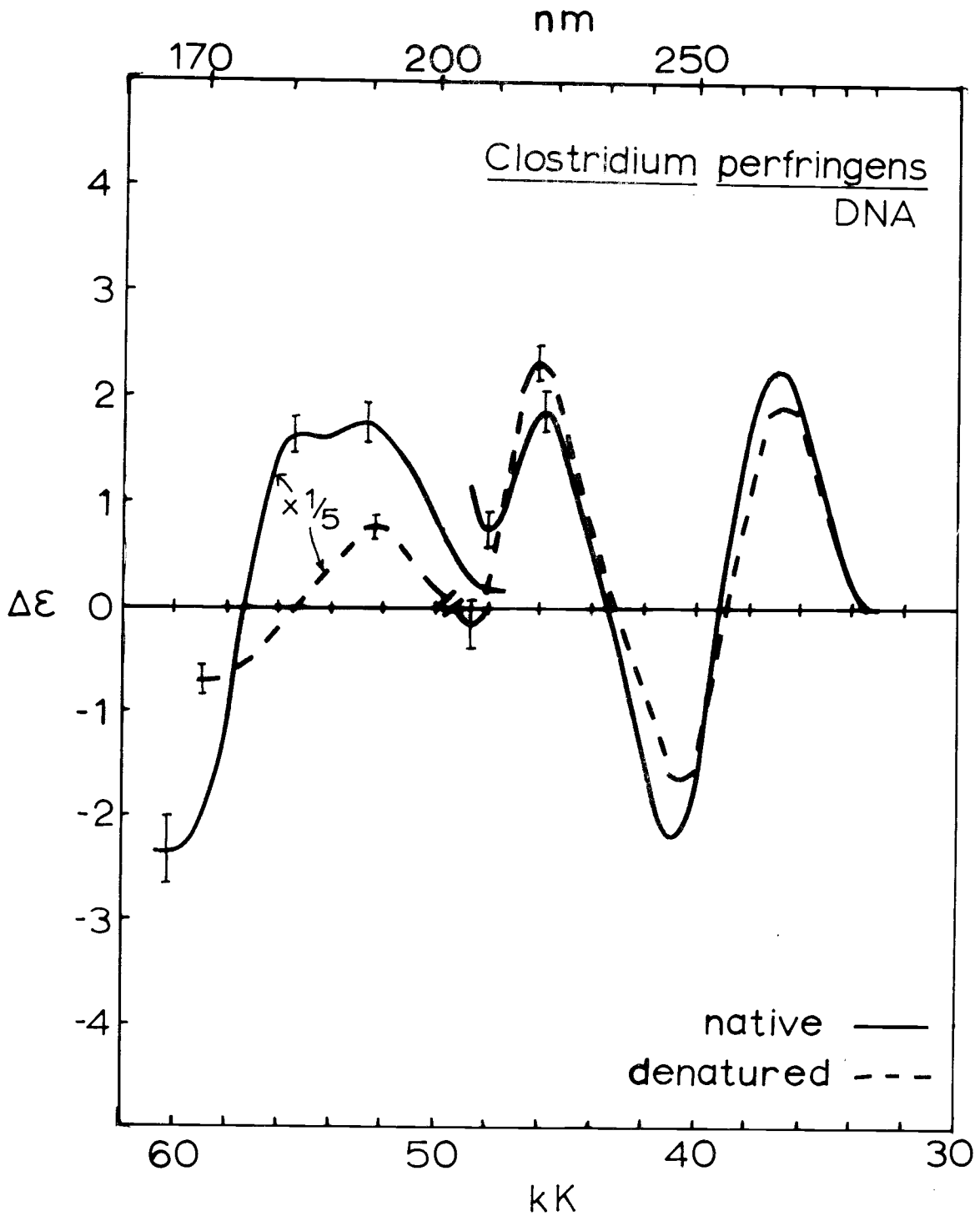


Figure 2. Measured circular dichroism for aqueous solutions of native (——) and heat denatured (---) C. perfringens D.N.A.

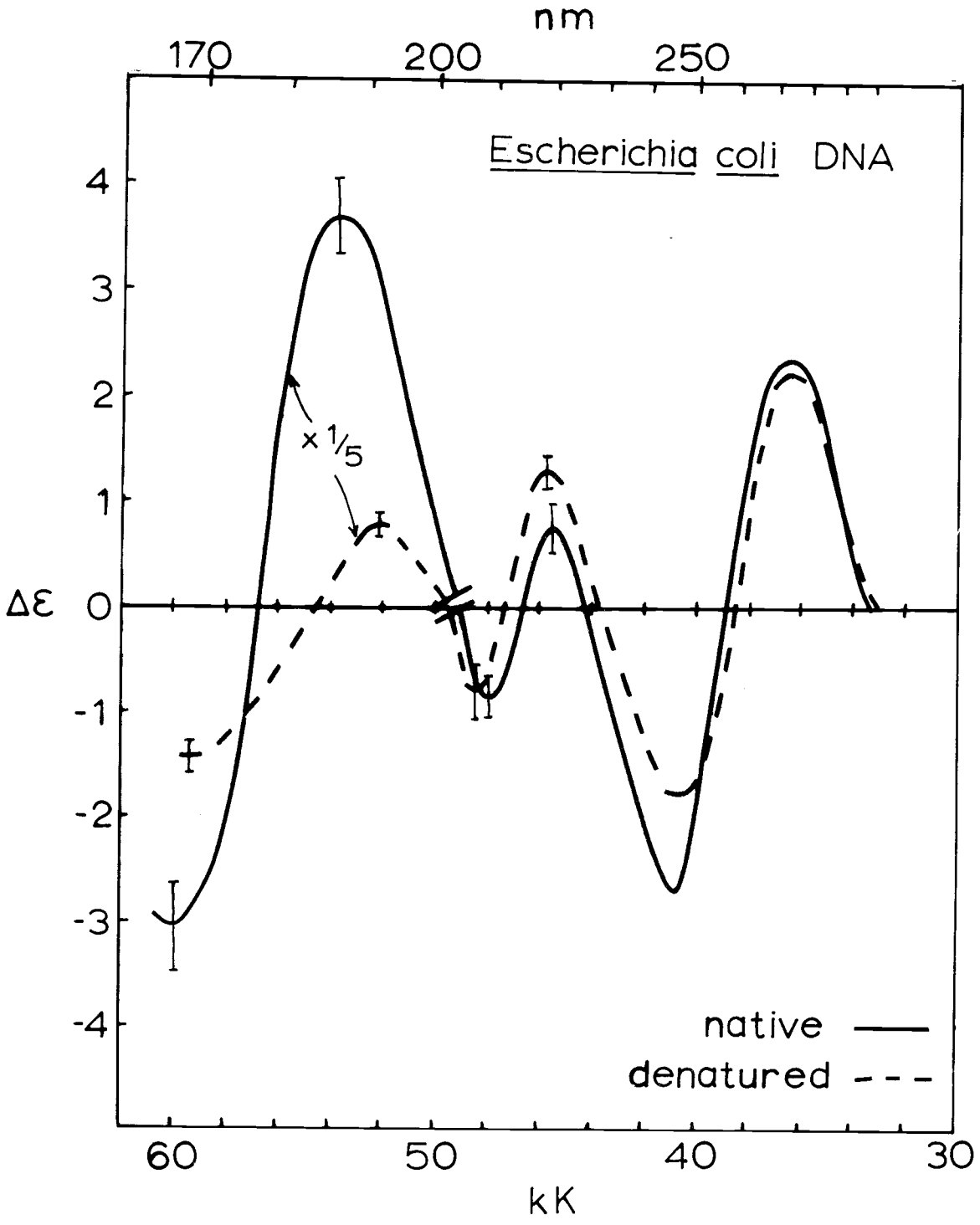


Figure 3. Measured circular dichroism for aqueous solutions of native (——) and heat denatured (- - -) E. coli D.N.A.

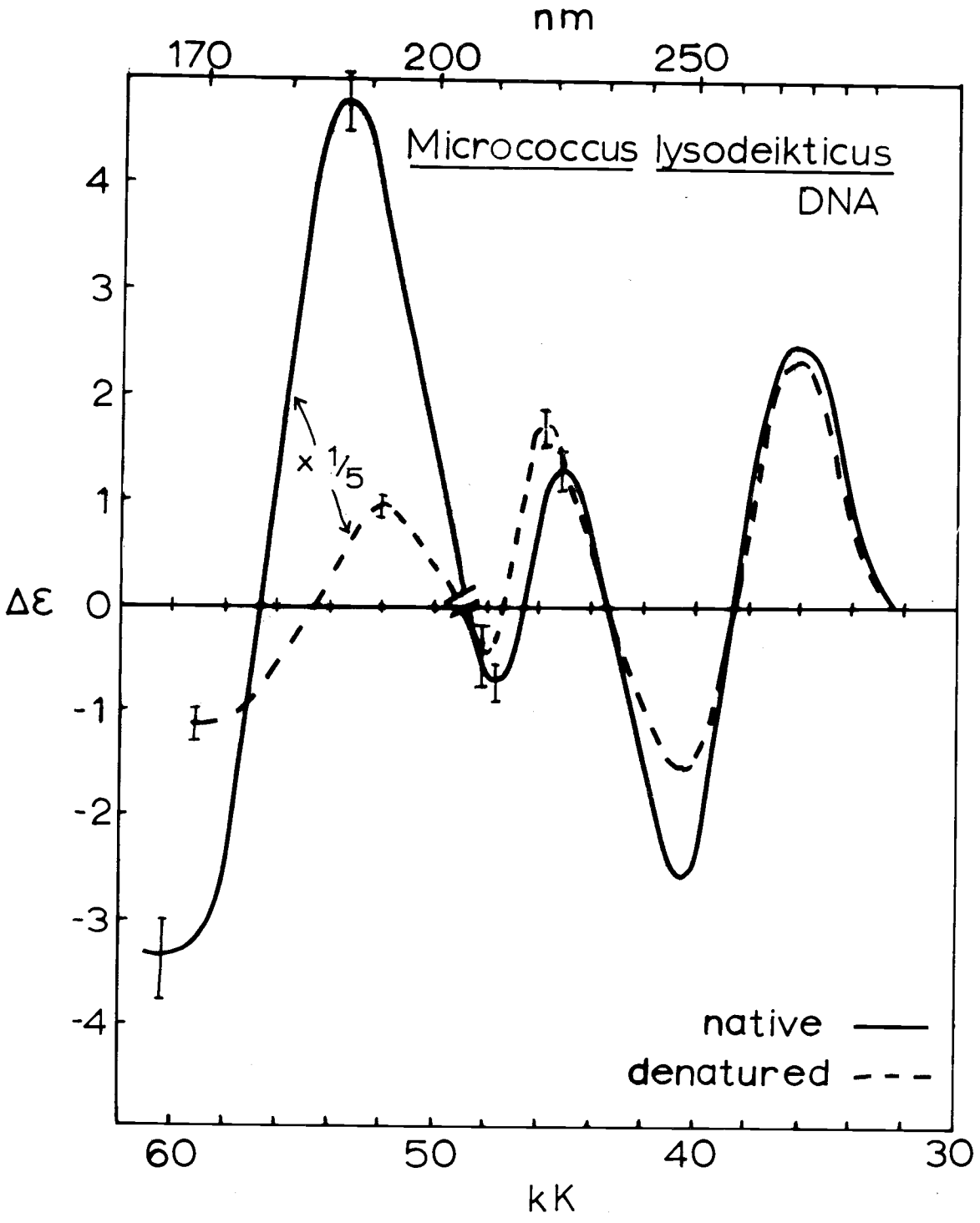


Figure 4. Measured circular dichroism for aqueous solutions of native (——) and heat denatured (- - -) M. lysodeikticus D.N.A.

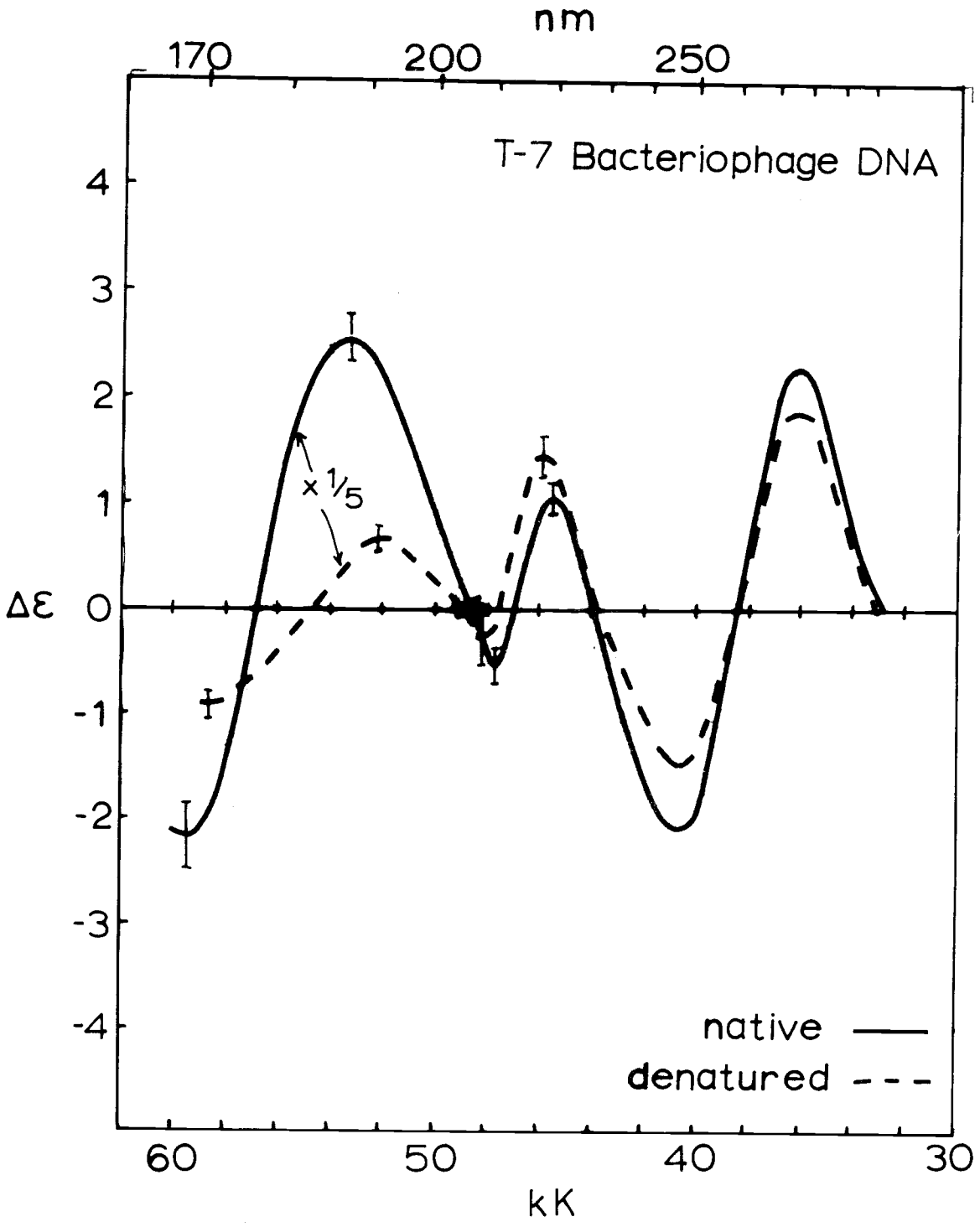


Figure 5. Measured circular dichroism for aqueous solutions of native (——) and heat denatured (- - -) bacteriophage T7 D.N.A.

The vacuum ultra violet spectrum of each of the native DNA's has an intense positive band at about 188 nm and an intense negative band at about 168 nm. The vacuum ultra violet portion of the spectrum has been scaled down by a factor of 1/5. For each of the native DNA's, the cut off point lies below the 168 nm band, so that the extremum of that band is fully passed.

The vacuum ultra violet spectrum of each of the heat denatured DNA's has a positive band at about 191 nm and a negative band at about 171 nm. Because of a red shift in the absorption spectrum of water upon heating, the cut off points of the denatured DNA's are lower in energy. In all of the heat denatured spectra except for calf thymus DNA it can be said with certainty only that the high energy end is terminated by an inflection in the slope. However, the circular dichroism spectrum of denatured calf thymus DNA is seen to extend beyond the extremum.

The two peaks in the vacuum ultra violet are strikingly reduced in magnitude upon heat denaturation. The first two bands in the near ultra violet are relatively insensitive by comparison. The magnitude of the third band increases upon heat denaturation for each of the five DNA's. The erratic behavior of the fourth band upon denaturation can be attributed to the fact that for each of theDNA's it is a band of small magnitude which is affected by the strong 188 nm band.

Inspection of the spectra in the vacuum ultra violet region reveals that there are significant differences in magnitude and shape for the various DNA's. Indeed, the 188 nm band is resolved into two peaks in the case of Clostridium perfringens DNA. It is well known that the circular dichroism spectrum of any DNA is determined by its sequence and conformation. Therefore the large differences in the circular dichroism among the various DNA's means that these bands are extremely sensitive to these attributes. For DNA's of the same conformation, the sequence information alone accounts for the differences among the spectra (Allen et al., 1972). Conversely, empirically established sequence spectra relationships would be expected to differ for DNA's of varying conformations. The vacuum ultra violet region of the circular dichroism spectrum should prove effective as a tool in the investigation of DNA sequence and conformation using both empirical and theoretical approaches.

## Acknowledgements

The authors wish to express appreciation to Dr. Kensal Van Holde for allowing us to use his Durrum Jasco Model J-10 circular dichroism spectrophotometer; to Dr. Irvin Isenberg for supplying us with the T-7 bacteriophage DNA; and to Mr. Richard Nelson for his stimulating discussions. This work was supported by NSF Grant GB-28960X.

## References


Allen, F.S., Gray, D.M., Roberts, G.P., Tinoco, I. (1972) Biopolymers 11, 853.

Brahms, J. & Mommaerts, W.F.H.M. (1964) J. Mol. Biol. 10, 73.

Felsenfeld, G. & Hirschman, S.Z. (1965) J. Mol Biol. 13, 407.

Fresco, J.R. (1961a) Tetrahedron 13, 185

Fresco, J.R., Lesk, A.M., Gorn, R., & Doty, P. (1961b) J. Am. Chem. Soc. 83, 3155.

Gennis, R.B. & Cantor, C.R. (1972) J. Mol. Biol. 65, 381.

Johnson, W.C. Jr. (1971) Rev. Sci. Instruments 42, 1283.

Jones, W. (1908) J. Biol. Chem. 5, 1

Li, H.J., Isenberg, I. & Johnson, W.C. Jr. (1971) Biochemistry 10, 2587

Marmur, J. & Doty, P. (1962) J. Mol. Biol. 5, 109.

Sarkar, P.K., Wells, B., & Yang, J.T. (1967) J. Mol. Biol. 25, 563.

Shatkin, A.J. (1969) Fundamental Techniques of Virology, Ed. by Habel, K. & Salzman, N.P. (Academic Press), p. 231.

Tunis-Schneider, M-J., B. & Maestre, M.F. (1970) J. Mol. Biol. 52, 543.

Wooley, S-Y. & Holzworth, G. (1971) J. Am. Chem. Soc. 93, 4066.